International Journal of

Cancer Therapy and Oncology

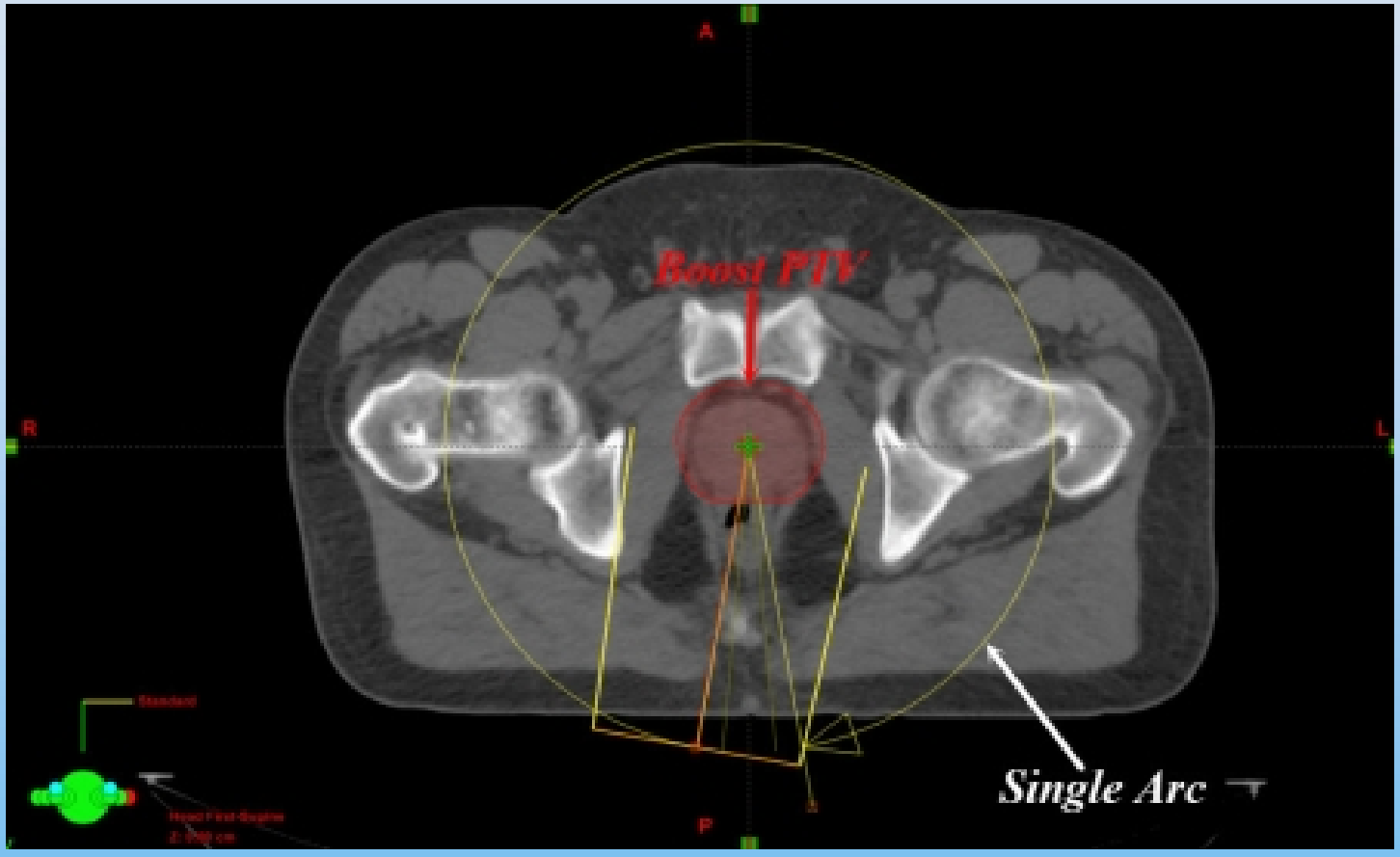

Volume 1, Number 1

(*October 2013*)

www.ijcto.org

ISSN 2330-4049

Editorial Board

TABLE OF CONTENTS

Editorials

Original Articles

Review Article

Scientific Notes

(The image used in this issue cover is from **Pokharel.** **DOI:10.14319/ijcto.0101.1**)

International Journal of Cancer Therapy and Oncology
www.ijcto.org

Notes of the editorial board on the role of medical physics in radiotherapy

Waldemar Ulmer

Klinikum München-Pasing, Department of Radiation Therapy and MPI of Physics, Göttingen, Germany

Received September 7, 2013; Accepted September 8, 2013; Published Online September 09, 2013

Editorial

The radiotherapy of malignant diseases has reached much progress during the past decade. Thus, intensity modulated radiation therapy (IMRT), RapidArc and Stereotaxy now belong to the standard modalities of tumor treatment with high energy radiation in clinical practice. In recent time, the particle therapy with protons and partially with heavy carbon ions has reached an important completion of these modalities with regard to some suitable applications. In spite of this enrichment essential features need further research activities and publications in this field: Nuclear reactions and the role of the released neutrons; electron capture of positively charged nuclei at lower projectile energies (e.g. in the environment of the Bragg peak and at the distal end of the particle track); correct dose delivery in scanning methods by accounting for the influence of the lateral scatter of beamlets.[1–7] Deconvolution methods can help to overcome these problems[4] ,which already occur in radiotherapy of very small photon beams.[8]

With regard to studies of clinical/radiobiological implications the accurate knowledge of the described problems is an essential feature and starting point. We particular mention the influence of released neutrons and the electron capture to the LET and RBE. In particular, electron capture of heavy ions such as carbon influences many aspects of this therapy modality and the superiority of these ions is drastically reduced in the domain of the Bragg peak.[3] Figures 1 – 3 make apparent the influence of electron capture for heavy carbon ions. Thus, all positively charged projectile show in the high energy domain a stripping effect, i.e. the charged projectile captures a surrounding electron, but this electron goes lost before a transition to a free shell can occur (Barkas effect). Only at lower projectile velocities the transition can occur.

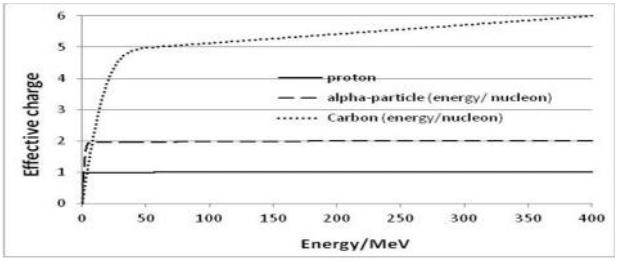

FIG. 1: Effective charge of the projectile nuclei proton, α-particle and carbon. The initial energy amounts to 400 MeV/nucleon.

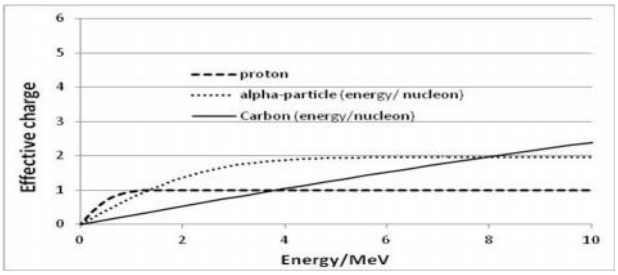

FIG. 2: Effective charge of the three projectile nuclei in the low energy region of Figure 1.

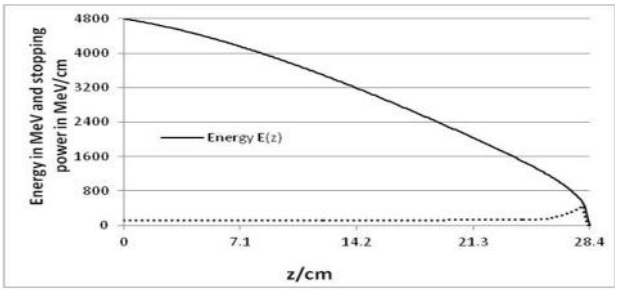

FIG. 3: E(z) versus dE/dz of a carbon ion in dependence of the depth z; the initial energy amounts to 400 MeV/nucleon.
(With regard to the Figures 1 – 3 it should be mentioned that independent of the initial energy (e.g 500 MeV/nucleon or 300 MeV/nucleon) the initial charge of the impinging carbon ion is always q = 6+. The publication [3] also presents effective charges q(E) of carbon ions with different initial energy.)

Corresponding author: Waldemar Ulmer, PhD; Klinikum München-Pasing, Department of Radiation Therapy and MPI of Physics, Göttingen, Germany;
Email: Waldemar.Ulmer@gmx.net

Cite this article as:
Ulmer W. Notes of the editorial board on the role of medical physics in radiotherapy. *Int J Cancer Ther Oncol* 2013;**1**(1):01014.
DOI: 10.14319/ijcto.0101.4

ISSN 2330-4049

In the case of carbon ions we have to consider a cascade of transitions to free atomic shells of carbon. At first, $(C_{6+})^{12}$ will be changed to $(C_{6,5+})^{12}$, and this electron capture effect is repeated, until the carbon ion is transformed to $(C_{6,1+})^{12}$ in the Bragg peak domain. At the distal end we obtain neutral carbon (or helium or hydrogen). Thus in the Bragg peak region the difference between the three projectile nuclei is rather small. Compared to protons the significantly increased importance of nuclear reactions and related fission products of carbon ions represents a further rather unresolved problem in the case of heterogeneous media. Contributions to these aspects can be found in the publications below, which should stimulate other authors to consider further research projects in this field.

References

1. Ulmer W, Matsinos E. Theoretical methods for the calculation of Bragg curves and 3D distribution of proton beams. *Eur Phys J Special Topics* 2010; **190**: 1-81.
2. Ulmer W, Schaffner B. Foundation of an analytical proton beamlet model for inclusion in a general proton dose calculation system. *Radiation Physics and Chemistry* 2011; **80**: 378–402.
3. Ulmer W. The role of electron capture and energy exchange of positively charged particles passing through matter. *Journal of Nuclear and Particle Physics* 2012; **2**: 77-86.
4. Ulmer W. Deconvolution of a linear combination of Gaussian kernels by Liouville-Neumann series applied to an integral equation of second kind with applications to radiation physics/image processing. *An Introductory Guide to Digital Image Processing (Edited by: A. Mishra)*. iConcept Press ISBN: 978-14775548-0-7 (2012).
5. Paganetti H. Nuclear interactions in proton therapy: dose and relative biological effect distributions originating from primary and secondary particles. *Phys Med Biol* 2002; **47**: 747-62.
6. Gottschalk B, Platais R,Platais H. Nuclear interactions of 160 MeV protons stopping in copper: A test of Monte Carlo nuclear models. MedPhys1999; **26**:2597 – 2601.
7. Zhang R, Newhauser W. Calculation of water equivalent thickness of materials of arbitrary density, elemental composition and thickness in proton beam irradiation. *Phys Med Biol* 2009; **54**: 1383-95.
8. Fan Y, Nath R. Intensity modulation under geometrical uncertainty: a deconvolution approach to robust fluence. *Phys Med Biol* 2010; 55:4029-45.

(Dr. W. Ulmer is an editorial board member of International Journal of Cancer Therapy and Oncology)

ISSN 2330-4049

International Journal of Cancer Therapy and Oncology
www.ijcto.org

Clinical implementation of radiobiological measures in treatment planning. Why has it taken so long?

Panayiotis Mavroidis [1, 2]

[1]*Cancer Therapy and Research Center, University of Texas Health Science Center, San Antonio, Texas, USA*
[2]*Karolinska Institutet and Stockholm University, Stockholm, Sweden*

Received September 29, 2013; Revised September 30, 2013; Accepted September 30, 2013; Published Online October 2, 2013

Editorial

It has been at least three decades since radiobiological models based on dose volume histograms (DVH) or 3-dimensional dose distributions started appearing in the literature as means to evaluate and compare radiotherapy treatment plans. Since then, many studies have shown that radiobiological treatment plan evaluation provides a closer association of the delivered treatment with the clinical outcome. This is achieved by taking into account the dose-response characteristics of the irradiated targets and normal tissues involved. In radiobiological treatment planning, biological tissue information and physical data have a complementary relation in analyzing dose plans due to the fact that both are incorporated in the mathematical expressions of the radiobiological models.

However, although the necessity of using radiobiological models in radiotherapy has been proven, their clinical implementation until now is almost negligible. Even the biological effective dose (BED) that was introduced in the early 80s has mainly been used to associate the maximum BED values of certain tissues with the respective risk for complications. And even though it has become a common knowledge that BED is a more accurate descriptor of the biological effectiveness of the applied physical dose, its clinical use is still limited. It is only during the recent years that BED started being used for dose prescription purposes instead of the physical dose or for determining BED-related dose thresholds for normal tissues. Furthermore, although the different treatment planning systems (TPS) have recently implemented the calculation of BED values, they still do not provide BED volume histograms or 3-dimenstional BED distributions or iso-BED line charts or the possibility of calculating the composite BED values in treatments composed by multiple phases. Usually, the clinical implementation of a new concept in radiotherapy is the result of the synergetic action between the clinical need and the availability of the relevant tools by the different TPSs.

The facts described above for the BED concept to a large extent hold for the clinical implementation of radiobiological models, namely the models that estimate the tumor control probability (TCP), normal tissue complication probability (NTCP) and complication-free tumor control probability (P_+). These models use radiobiological parameters that describe the dose-response relations of the different tumors and normal tissues. The derivation of the model parameters can be performed by different means such as a maximum likelihood fitting using a cohort of patients for whom the delivered 3-dimensional dose distributions and fractionation scheme as well as the relevant treatment related organ responses have been registered. Although radiobiological models use the complete dosimetric information of a given treatment plan in order to quantify its quality, in clinical practice dose prescription and treatment plan evaluation are based on single doses in the tumor, mean physical doses to the PTV or physical dose-volume points to the tumor and involved organs at risk (OARs), which however take into account a fraction only of the treatment information. Furthermore, the values of those treatment plan quality descriptors are usually characterized by large uncertainty intervals, which however are not taken into account clinically.

The current status of treatment planning practice is the result of the traditional approach of using dosimetric descriptors for quantifying the quality of treatment plans and the fact that the values of these descriptors could be calculated by the TPS, which made their clinical implementation easier. However, all these descriptors are indirectly related

Corresponding author: Panayiotis Mavroidis, PhD; Division of Medical Physics, Department of Radiation Oncology, University of Texas Health Science Center, San Antonio, Texas USA; Email: mavroidis@uthscsa.edu

Cite this article as:
Mavroidis P.Clinical implementation of radiobiological measures in treatment planning. Why has it taken so long? Int J Cancer Ther Oncol 2013;1(1):01019. **DOI:** 10.14319/ijcto.0101.9

ISSN 2330-4049

with treatment plan quality and they do not answer to the fundamental questions of 'what if the likelihood to achieve tumor control' or 'what is the likelihood to have side effects to the OARs' when evaluating a given treatment plan. These answers are provided by the TCP and NTCP measures irrespective of the treatment technique, cancer site, fractionation scheme or clinical protocol applied. So, although radiobiological models convey to a larger extent the clinical insight and the values of their parameters are more accurate compared to those of the descriptors that are used clinically, their clinical implementation is negligible.

There are two main reasons for this. First, there is lack of understanding the theory and the basic concepts behind radiobiological modeling by many radiation oncologists. It can be easily shown that the classes devoted to radiobiological modeling either during the university studies or during the medical residency programs are very limited in number and extent. Second and more important, is the fact that only recently some TPS started offering some tools for performing radiobiological evaluation and comparison of different treatment plans. But still this is not adequate because in order these tools to be used clinically, one has to reach the point of having established radiobiological treatment planning as a clinically implemented procedure.

In order to reach this point, the different TPS should offer to the clinician's tools that will help them organize their patient treatment information and follow-up registrations in order to enable them determine the values of the radiobiological parameters of the models they want to use, based on their own patient data. Appropriate tools should be offered for performing clinical verification of such clinically derived parameter values as well as for performing clinical validation of parameter sets found in the literature. By using those tools, patient datasets consisting of individual tissue response and dose distribution data can be fitted by different radiobiological models and their goodness-of-fit can be evaluated. These are the important elements that are missing for a clinical implementation of radiobiological modeling, the absence of which has led to this long delay in seeing a reasonable progress in this issue.

Radiobiological treatment plan evaluation may allow a fairly accurate prediction of tumor control or normal tissue complications taking into account the variations in patient radiosensitivity. The use of radiobiological modeling is necessary if a clinically relevant quantification of a dose plan is needed.

(Dr. Panayiotis Mavroidis is an editorial board member of International Journal of Cancer Therapy and Oncology)

 ISSN 2330-4049

International Journal of Cancer Therapy and Oncology
www.ijcto.org

MRI and DWI: the future in cervical cancer?

Daniel Grossi Marconi*, Erick Rauber, Paula de Cassia Soares

Department of Radiation Oncology, Barretos Cancer Hospital, Barretos/SP, Brazil

Received September 24, 2013; Revised September 26, 2013; Accepted September 27, 2013; Published Online September 27, 2013

Editorial

Cervical cancer is the third leading cause of female cancer worldwide and is the second most common cause of cancer related deaths in women in undeveloped countries.[1] The incident rate varies with the prevalence of risk factors and the lack of adequate screening programs, reaching 80 cases per 100,000 inhabitants in Recife, Brazil.[2] Despite advances in treatment, cervical cancer still maintains high rates of morbidity and mortality – the recurrence rate and associated death is approximately 30%. Data from the UK show that one third of patients will die within 5 years of diagnosis. [3] For all these reasons cervical cancer can be considered a public health issue especially in developing countries.

The International Federation of Gynecology and Obstetrics (FIGO) stage system is the most widely used for cervical cancer. This system emphasizes the clinical parameters at the expense of morphological and functional examinations, which facilitates its applicability in developing countries - where additional tests are expensive and not available. The main limitations are the fact that this system is examiner dependent, difficult to reproduce, and difficult to perform in obese patients or those with unfavorable anatomy.

Although without altering the classification proposed by FIGO, exams are valuable in this disease as they tend to guide the practitioner toward more accurate treatment. Furthermore, they are important to assess the response to treatment, which is of paramount importance since additional therapies (i.e. hysterectomy) may be used in cases of persistent disease.

The 18-FDG PET stands out as the most used and studied functional test in cervical cancer. Unfortunately, PET is not available to many treatment centers around the world, especially in those that have the highest incidence rates – as the funds needed to obtain its tracer make it cost prohibitive.

In this context, a much more cost effective relation is the MRI. Stenstedt *et al.* [4] studied the impact of MRI in staging and follow-up of cervical lesions and concluded that the addition of this examination alter the staging proposed by FIGO and changes the treatment plan in many cases. In 2013, Kraljevic *et al.* [5] performed a study comparing the FIGO staging and MRI preoperatively and correlated these findings with the pathological outcome in patients treated surgically. They concluded that MRI is better than clinical staging (accuracy of 90.9% versus 79.0%).[5]

Novel advances such as diffusion weighted image (DWI) (sequence that is sensitive to the random motion of water molecules - i.e., Brownian motion) allow us to evaluate changes during therapy. Restriction to this diffusion movement is directly associated to the degree of cellularity of the tissue and thus is related to primary malignancy and metastasis.[6] An actual issue is whether its changes are predictive of response: the DWI derived apparent diffusion coefficient (ADC) is capable to quantify the magnitude of this water diffusion and has been used extensively as a biomarker for therapeutic response in many cancer types.

Emerging studies seek to consolidate the actual role of MRI and their different weights in the staging and therapeutic monitoring of cervical cancer. Advantages such as cost-effectiveness (pathology is predominant in developing countries) and absence of need of contrast (essential in cases where there is impairment of renal function) add to this exam key features to this pathology. It is not difficult to predict that if new studies demonstrate in practice these advantages, MRI/DWI could be considered essential in the future.

*Corresponding author: Daniel Grossi Marconi, Department of Radiation Oncology, Barretos Cancer Hospital, Barretos/SP, Brazil. Email: dgmarconi@gmail.com

Cite this article as:
Marconi D, Rauber E, Soares P. MRI and DWI: the future in cervical cancer? Int J Cancer Ther Oncol 2013;1(1):01018.
DOI: 10.14319/ijcto.0101.8

ISSN 2330-4049

References

1. Ferlay J, Shin HR, Bray F, Forman D, Mathers C, Parkin DM. GLOBOCAN (2008) Cancer incidence and mortality worldwide. *International Agency for Research on Cancer, Lyon*. 2010; **127**: 2893-2917. CrossRef

2. Jemal A, Siegal R, Xu J, Ward E. Cancer Statistics, 2010. *CA Cancer J Clin* 2010; **60**: 277-300. CrossRef

3. *Cancer Research UK* (2010) Cervical cancer: survival statistics. Available via http://info.cancerresearchuk.org/cancerstats Accessed on September 21, 2013.

4. Stenstedt K, Hellström AC, Fridsten S, Blomqvist L. Impact of MRI in the management and staging of cancer of the uterine cervix. *Acta Oncol* 2011; **50**:420-426. CrossRef

5. Kraljević Z, Visković K, Ledinsky M, Zadravec D, Grbavac I, Bilandzija M, Soljacić-Vranes H, Kuna K, Klasnić K, Krolo I. Primary uterine cervical cancer: correlation of preoperative magnetic resonance imaging and clinical staging (FIGO) with histopathology findings. *Coll Antropol* 2013; **37**:561-568.

6. Malayeri AA, El Khouli RH, Zaheer A, Jacobs MA, Corona-Villalobos CP, Kamel IR, Macura KJ. Principles and applications of diffusion-weighted imaging in cancer detection, staging, and treatment follow up. *Radiographics* 2011; **31**:1773-1791. CrossRef

 ISSN 2330-4049

International Journal of Cancer Therapy and Oncology
www.ijcto.org

Dosimetric impact of mixed-energy volumetric modulated arc therapy plans for high-risk prostate cancer

Shyam Pokharel

Department of Medical Physics, Premier Oncology, Fort Myers, Florida, USA

Received August 02, 2013; Revised August 29, 2013; Accepted August 31, 2013; Published Online August 31, 2013

Original Research

Abstract

Purpose: This study investigated the dosimetric impact of mixing low and high energy treatment plans for high prostate cancer treated with volumetric modulated arc therapy (VMAT) technique in the form of RapidArc. **Methods:** A cohort of 12 prostate cases involving proximal seminal vesicles and lymph nodes was selected for this retrospective study. For each prostate case, the single-energy plans (SEPs) and mixed-energy plans (MEPs) were generated. First, the SEPs were created using 6 mega-voltage (MV) energy for both the primary and boost plans. Second, the MEPs were created using 16 MV energy for the primary plan and 6 MV energy for the boost plan. The primary and boost MEPs used identical beam parameters and same dose optimization values as in the primary and boost SEPs for the corresponding case. The dosimetric parameters from the composite plans (SEPs and MEPs) were evaluated. **Results:** The dose to the target volume was slightly higher (on average <1%) in the SEPs than in the MEPs. The conformity index (CI) and homogeneity index (HI) values between the SEPs and MEPs were comparable. The dose to rectum and bladder was always higher in the SEPs (average difference up to 3.7% for the rectum and up to 8.4% for the bladder) than in the MEPs. The mean dose to femoral heads was higher by about 0.8% (on average) in the MEPs than in the SEPs. The number of monitor units and integral dose were higher in the SEPs compared to the MEPs by average differences of 9.1% and 5.5%, respectively. **Conclusion:** The preliminary results from this study suggest that use of mixed-energy VMAT plan for high-risk prostate cancer could reduce the integral dose and minimize the dose to rectum and bladder, but for the higher femoral head dose.

Keywords: Prostate Cancer; Mixed Energy Plan; VMAT; RapidArc

Introduction

In external beam radiation therapy, treatment techniques such as 3-dimensional conformal therapy (3DCRT), intensity modulated radiation therapy (IMRT), and volumetric modulated arc therapy (VMAT) are generally used to treat prostate cancer with an objective of delivering conformal dose distributions to the target while minimizing the doses to the normal tissues. Since prostate cancer involves the deep-seated target, the high-energy photon beams are generally used for 3DCRT due to their greater penetrating power.[1]

Corresponding author: Shyam Pokharel, PhD; Premier Oncology, 4571 Colonial Blvd, Unit 100, Fort Myers, FL 33966, USA; Email: pokharel@livemail.uthscsa.edu

Cite this article as:
Pokharel S. Dosimetric impact of mixed-energy volumetric modulated arc therapy plans for high-risk prostate cancer. Int J Cancer Ther Oncol 2013;1(1):01011. **DOI**: 10.14319/ijcto.0101.1

However, the photon beams with energy 10 mega-voltage (MV) or higher also create the secondary neutrons due to interaction between the photons and treatment head of the machine.[1] Despite high-energy photon having an advantage in penetrating power and skin sparing, use of lower energy (6–10 MV) photon beams have been found to be an effective energy choices for the majority of IMRT prostate cases.[1,2] Furthermore, several studies demonstrated no clear dosimetric advantages using high-energy photon beams for IMRT prostate cases when compared to the low-energy photon beams.[2-8]

Recently, Park *et al.*[8] investigated the effect of changing beam energy according to the penetration depths on the quality of IMRT plans for prostate cancer and made the comparisons between mixed-energy plans (MEPs) and single-energy plans (SEPs) of either low or high energy. In that study[8], Park *et al.* showed that mixing energy in an IMRT plan for deep-seated tumors could improve the overall plan quality. However, the dosimetric impact of MEPs for pros-

ISSN 2330-4049

tate cancer using VMAT technique remains to be addressed. Thus, we investigated the effect of mixing the low energy (6 MV) and high energy (16 MV) treatment plans for prostate cancer treated with VMAT technique in the form of RapidArc (Varian Medical Systems, Palo Alto, CA, USA). The dosimetric comparisons between SEPs and MEPs were done for 12 prostate cases.

Methods and Materials

A cohort of 12 prostate cases involving proximal seminal vesicles and lymph nodes was selected for this retrospective study. All 12 cases were treated with RapidArc technique at Premier Oncology, Fort Myers. Florida, USA. The computed tomography (CT) simulation of patients was performed in a supine position on the Phillips Brilliance CT Scanner (Philips Healthcare, Andover, MA, USA), and the CT images were acquired with a 3 mm spacing. The contouring of prostate, proximal seminal vesicles, lymph nodes, and organs at risk (OARs) (rectum, bladder, and femoral heads) was done on the axial slices of the CT in the Eclipse treatment planning system (TPS), version 11.1 (Varian Medical Systems, Palo Alto, CA, USA). The primary clinical target volume (CTV_p) was defined as the prostate, seminal vesicles, and lymph nodes, whereas the boost clinical target volume (CTV_b) was defined as the prostate only. The primary and boost planning target volume (PTV_p and PTV_b, respectively) was generated with a margin of 7 mm around the CTV_p and CTV_b, respectively, in all directions except in the posterior direction, where a margin of 0.5 cm was used.

The RapidArc treatment plans of all 12 cases were generated in the Eclipse TPS using 6 and 16 MV X-ray beams Varian Clinac iX (Varian Medical Systems, Palo Alto, CA, USA). Each treatment plan consisted of primary and boost plan, and the total prescription dose was 81 Gy with a daily dose of 1.8 Gy over 45 fractions. Furthermore, the prescription dose to the primary plan was 45 Gy to the PTV_p, and the prescription dose to the boost plan was 36 Gy to the PTV_b. For each prostate case, the SEPs and MEPs were generated.

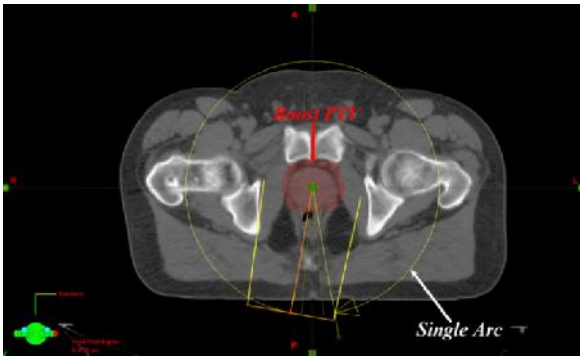

FIG. 1: A transversal view of VMAT (RapidArc) plan set up for boost PTV (case #7) using one arc in Eclipse treatment planning system. Abbreviations: VMAT = volumetric modulated arc therapy, PTV = planning target volume.

First, the SEPs were created using a 6 MV photon beam for both the primary plan and separate boost plan. The treatment plan was set up using one, two or three arcs depending on the size of the target volume. [Figure 1] The length of gantry rotations, collimator angle, and field sizes of the coplanar arcs for the primary as well as boost plans were chosen based on the location of the PTV and OARs using the beam-eye-view (BEV) graphics. [Figure 2]

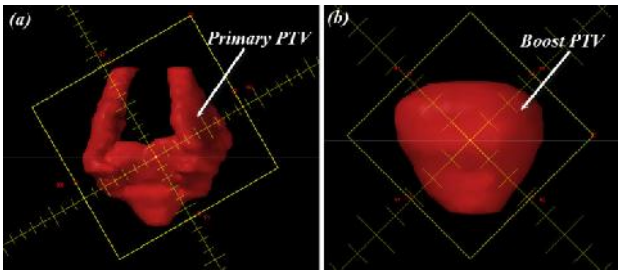

FIG. 2: Beam's-eye-view of case #7 showing (a) primary planning target volume (PTV), and (b) boost PTV in the Eclipse treatment planning system.

The isocenter of the plan was placed at the center of the target volume (i.e., PTV_p or PTV_b). The primary and boost plans were optimized using Progressive Resolution Optimizer (PRO) (version 11.1). The dose-volume constraints and their weightings were adjusted during the optimization process of SEPs such that at least 95% of the target volume was covered by the prescription dose while keeping the dose to the OARs as minimum as possible. The plan optimization process was carried out with an objective of meeting the planning criteria listed in Table 1.

TABLE 1: Dose specifications for rectum, bladder, and femoral heads in the composite plan

Organ Limit*	$D_{15\%}$	$D_{25\%}$	$D_{35\%}$	$D_{50\%}$
Rectum	< 75 Gy	< 70 Gy	< 65 Gy	< 60 Gy
Bladder	< 80 Gy	< 75 Gy	< 70 Gy	<65 Gy
Femoral	Mean Dose < 45 Gy			

*Normal organ limit refers to the volume of that organ that should not exceed the dose limit. Abbreviation: $D_{x\%}$ = Dose received by x% of total OAR volume, where x % = 15, 25, 35 and 50; OAR = Organ at risk.

Second, the MEPs were created using a 16 MV photon beam for the primary plan and a 6 MV photon beam for the boost plan. Specifically, the primary MEP used the identical beam parameters and same optimization dose-constraints and their weightings as in the final primary SEP plan for the corresponding case. Similarly, the boost MEP and boost SEP had the same beam parameters and plan optimization values for the corresponding case. No modifications of dose-volume constraints and weightings were made during the optimization processes of MEPs.

The optimized SEPs and MEPs plans were calculated with the anisotropic analytical algorithm (AAA), version 11.1, using dose calculation grid size of 2.5 mm. All calculated

 ISSN 2330-4049

plans were then normalized such that at least 95% of the PTV volume was covered by the prescription dose. The primary and boost plans were combined to generate a composite (COMP) plan. This allowed us to perform the dosimetric comparison between the SEPs and MEPs using the dose-volume histograms (DVHs) of the COMP plans that were generated in the Eclipse TPS. The DVH parameters evaluated for the target volume (PTV_b) were: mean dose, maximum dose, conformity index (CI) defined as the ratio of volume of the isodose cloud receiving 100% of the prescription dose ($V_{100\%}$) to volume of the PTV_b, and homogeneity index (HI) defined as the ratio of dose at 5% of the PTV_b ($D_{5\%}$) to dose at 95% of the PTV_b ($D_{95\%}$). For rectum and bladder, the volumes that received 70 Gy, 40 Gy, and 20 Gy, (V_{70Gy}, V_{40Gy}, and V_{20Gy}, respectively) as well as mean dose were compared. The mean dose to the femoral heads was evaluated. In addition, the number of monitor units (MUs) and normal tissue integral dose were compared too.

For the purpose of comparison, the average percentage difference ($D_{avg.}$) between the SEPs and MEPs at the corresponding dosimetric parameter of the same case was calculated using Equation **1**.

$$D_{avg.}(x) = \frac{1}{12}\sum_{n=1}^{12}\left[\frac{(SEP)_n - (MEP)_n}{(SEP)_n}\times 100\right] \qquad \text{Eq.1}$$

where x is a corresponding dosimetric parameter in the COMP SEPs and MEPs for the n^{th} case. In Equation **1**, the $D_{avg.}$ is expressed in percentage and averaged over all twelve cases in this study. At a given dosimetric parameter, a positive $D_{avg.}$ means higher dosimetric value in the SEPs compared with the MEPs, and a negative $D_{avg.}$ means higher dosimetric value in the MEPs compared with the SEPs. The statistical analysis was done using paired two-sided student's t-test in a Microsoft Excel spreadsheet, and a p- value of less than 0.05 was considered to be statistically significant.

Results

Table 2 and Figures 3, 4, 5, and 6 summarize the dosimetric results in the COMP plans, and the values are averaged over the twelve analyzed cases. The dosimetric results obtained in this study were clinically acceptable.

The maximum and mean doses to the target volume were slightly higher in the SEPs than in the MEPs by an average difference of less than 1%, and the results showed the statistical significance with p-values of 0.001 and 0.044 for the maximum and mean dose, respectively. The CI and HI values between SEPs and MEPs were comparable with average differences of 1% for the CI (p = 0.009) and 0.4% for the HI (p = <0.000) showing statistical significance.

The dose to the rectum was always higher in the SEPs and

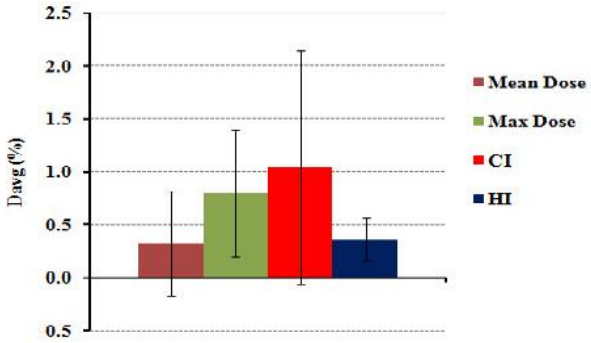

FIG. 3: The $D_{avg.}$ (%) between SEPs and MEPs for the PTV doses, CI, and HI. The values are averaged over the twelve analyzed cases. Note: The error bars represent the standard deviations. The $D_{avg.}$ (%) is defined in equation 1 (Materials and Methods). Abbreviations: $D_{avg.}$ = average difference, SEPs = single energy plans, MEPs = mixed energy plans, PTV = planning target volume, CI = conformity index, HI = homogeneity index.

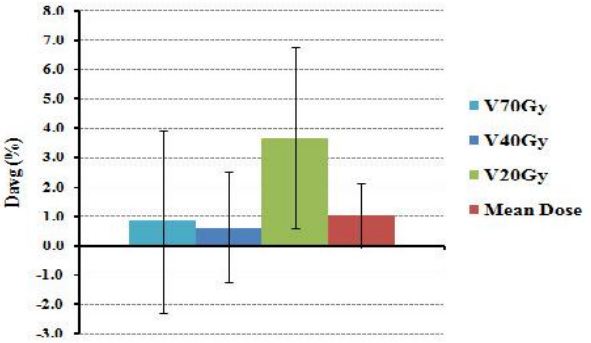

FIG. 4: The $D_{avg.}$ (%) between SEPs and MEPs for the V_{70Gy}, V_{40Gy}, V_{20Gy}, and mean does to the rectum. The values are averaged over the twelve analyzed cases. Note: The error bars represent the standard deviations. The $D_{avg.}$ (%) is defined in Equation 1 (Materials and Methods). Abbreviations: $D_{avg.}$ = average difference, SEPs = single energy plans, MEPs = mixed energy plans, V_{nGy} = percentage volume irradiated by n Gy or more of a certain structure

lower in the MEPs with an average difference ranging from 0.6% (at V_{40Gy}) to 3.7% (at V_{20Gy}). The statistical significance was obtained for the mean dose (p = 0.009) and V_{20Gy} (p = 0.003), whereas the statistical significance was not seen for the V_{70Gy} (p = 0.427) and V_{40Gy} (p = 0.277). Similar to the dosimetric results for the rectum, the dose to the bladder was higher in the SEPs and lower in the MEPs. However, the range of average difference values between the SEPs and MEPs were larger for bladder compared to the one for rectum. Specifically, the average difference values in bladder ranged from 0.1% (at V_{20Gy}) to 8.4% (at V_{40Gy}). Furthermore, the statistical significance was obtained for the mean dose (p <0.000), V_{70Gy} (p = 0.007), and V_{40Gy} (p = 0.002), whereas the results for V_{20Gy} (p = 0.384) were not statistically significant.

 ISSN 2330-4049

TABLE 2: Comparison of dosimetric parameters for the single and mixed energy composite (primary + boost) plans.

		SEP (Avg. ± SD)	MEP (Avg. ± SD)	*p-value*
PTV_b (127.2 ± 35.2 cc)	Mean Dose (Gy)	83.2 ± 0.4	82.9 ± 0.3	**0.044**
	Max. Dose (Gy)	86.3 ± 0.6	85.6 ± 0.6	**0.001**
	CI	1.09 ± 0.05	1.08 ± 0.05	**0.009**
	HI	1.03 ± 0.00	1.03 ± 0.00	**<0.000**
Rectum (77.6 ± 47.1 cc)	Mean Dose (Gy)	34.6 ± 3.9	34.3 ± 3.9	**0.009**
	V_{70Gy} (%)	6.5 ± 2.8	6.5 ± 2.8	0.427
	V_{40Gy} (%)	26.1 ± 7.0	25.9 ± 6.9	0.277
	V_{20Gy} (%)	89.3 ± 3.9	86.1 ± 13.2	**0.003**
Bladder (325.9 ± 218.2 cc)	Mean Dose (Gy)	43.2 ± 5.2	42.2 ± 5.0	**<0.000**
	V_{70Gy} (%)	9.3 ± 4.3	9.0 ± 4.1	**0.007**
	V_{40Gy} (%)	45.4 ± 17.2	41.4 ± 15.3	**0.002**
	V_{20Gy} (%)	99.8 ± 0.5	99.7 ± 0.8	0.384
Femoral Heads (135.7 ± 16.5 cc)	Mean Dose (Gy)	28.0 ± 3.8	28.2 ± 3.4	0.684
Monitor Units (MUs)		590 ± 35	538 ± 34	**<0.000**
Integral Dose (10^5 Gy-cc)		3.2 ± 0.5	3.0 ± 0.5	**<0.000**

Abbreviations: SEP = Single Energy Plan, MEP = Mixed Energy Plan, Avg. = Average, SD = Standard Deviation, PTV_b = Boost Planning Target Volume, Max. Dose = Maximum Dose, V_{nGy} = Percentage volume irradiated by n Gy or more of a certain structure, CI = Conformity Index, HI = Homogeneity Index. (The values are averaged over the 12 analyzed cases. The *p*-values were obtained from paired two-sided student's t-test. The p-values less than 0.05 were considered to be statistically significant).

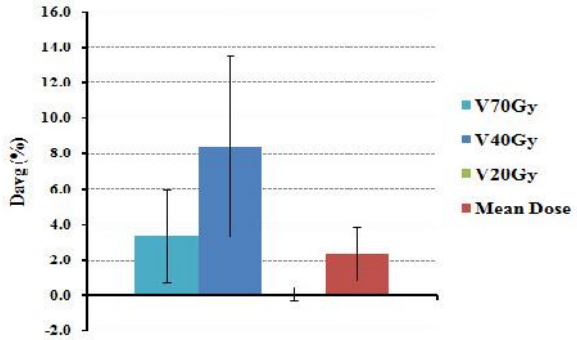

FIG. 5: The $D_{avg.}$ (%) between SEPs and MEPs for the V_{70Gy}, V_{40Gy}, V_{20Gy}, and mean does to the bladder. The values are averaged over the twelve analyzed cases. Note: The error bars represent the standard deviations. The $D_{avg.}$ (%) is defined in equation 1 (Materials and Methods). Abbreviations: $D_{avg.}$ = average difference, SEPs = single energy plans, MEPs = mixed energy plans, V_{nGy} = percentage volume irradiated by *n* Gy or more of a certain structure

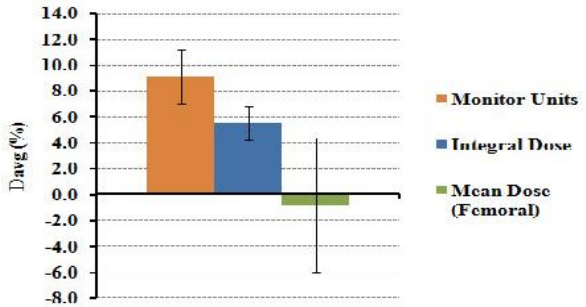

FIG. 6: The $D_{avg.}$ (%) between SEPs and MEPs for the femoral head mean dose, normal tissue integral dose, and MUs. The values are averaged over the twelve analyzed cases. Note: The error bars represent the standard deviations. The $D_{avg.}$ (%) is defined in equation 1 (Materials and Methods). Abbreviations: $D_{avg.}$ = average difference, SEPs = single energy plans, MEPs = mixed energy plans, MUs = Monitor Units.

In contrast to the results seen for the rectum and bladder in this study, the mean dose to the femoral heads was higher in the MEPs by an average difference of 0.8% with no statistical significance (p = 0.684). In comparison to the MEPs, the number of MUs and integral dose were higher in the SEPs by average differences of 9.1% (p < 0.000) and 5.5% (p < 0.000), respectively, showing the statistical significances.

Discussion

In this study, we investigated the dosimetric impact of mixing low energy (6 MV) and high energy (16 MV) treatment plans for prostate cancer treated with RapidArc technique. The results from this study showed no clear dosimetric differences between the SEPs and MEPs for the target volume. However, the results suggested that the use of mixed energy treatment plans for prostate cancer could potentially reduce the dose to the OARs, especially for bladder and rectum.

 ISSN 2330-4049

The use of lower energy photon beams generally minimizes the head leakage, internal scatter, and secondary neutrons.[2-7] However, the low-energy photon beams also requires greater number of MUs to deposit high doses in the area peripheral to the target, resulting increase in the integral dose and radiation exposure to the OARs.[4] The results in our study also showed that the number of MUs in the lower energy (6 MV) plans (i.e., SEPs) were about 9% higher (on average) in comparison to the MEPs that contained higher energy (16 MV) photon beam. Furthermore, the integral dose to the normal tissues was lower in the MEPs by about 5.5% (on average), and this would also reduce the radiation-induced secondary cancer. [9, 10]

The dosimetric differences in the treatment plans from the use of low and high energy photon beams depend on the beam modeling employed within the dose calculation algorithm.[11] In this study, we used AAA to calculate the dose in all treatment plans. Several studies[12-17] have documented the limitation of AAA in estimating the dose more accurately when heterogeneous media are involved along the photon beam path. Recently, a number of studies have shown that Acuros XB, new dose calculation algorithm employed within Eclipse TPS, is more accurate than AAA for photon dose calculation, especially in the heterogeneous media.[14-17] The dosimetric and radiobiological impact of Acuros XB on the prostate cancer treatment plans due to change in photon beam energy will be an interesting topic for future studies.

Conclusion

The preliminary results from this study suggest that use of mixed-energy VMAT plan for high-risk prostate cancer could reduce the integral dose and minimize the dose to rectum and bladder, but for the higher femoral head dose.

Competing interests

The authors declare that they have no competing interests.

References

1. NCRP. Report No, 79: Neutron contamination from medical electron accelerators. Bethesda, Maryland; *NCRP*. 1987.
2. Soderstrom S, Eklof A, Brahme A: Aspects on the optimal photon beam energy for radiation therapy. *Acta Oncol* 1999; **38**: 179–187.
3. Pirzkall A, Carol MP, Pickett B, Xia P, Roach M 3rd, Verhey LJ. The effect of beam energy and number of fields on photon-based IMRT for deep-seated targets. *Int J Radiat Oncol Biol Phys* 2002; **53**: 434–442.
4. Subramanian TS. Linear accelerators used for IMRT should be designed as small field, high intensity, intermediate energy units [For the proposition]. *Med Phys* 2002; **29**: 2526–28.
5. Söderstrom S, Eklöf A, Brahme A. Aspects on the optimal photon beam energy for radiation therapy. *Acta Oncol* 1999; **38**: 179–187.
6. Welsh JS, Mackie TR, Limmer JP. High-energy photons in IMRT: uncertainties and risks for questionable gain. *Technol Cancer Res Treat* 2007; **6**: 147–149.
7. Sun M and Ma L. Treatments of exceptionally large prostate cancer patients with low-energy intensity-modulated photons. *J Appl Clin Med Phys* 2006;**7**: 43–49.
8. Park JM, Choi CH, Ha SW, Ye SJ. The dosimetric effect of mixed-energy IMRT plans for prostate cancer. *J Appl Clin Med Phys* 2011;**12** :3563.
9. Brenner DJ, Curtis RE, Hall EJ, Ron E. Second malignancies in prostate carcinoma patients after radiotherapy compared with surgery. *Cancer* 2000; **88**: 398-406.
10. Hall EJ, Wuu CS. Radiation-induced second cancers: the impact of 3D-CRT and IMRT. *Int J Radiat Oncol Biol Phys* 2003; **56**: 83-88.
11. Madani I, Vanderstraeten B, Bral S, et al. Comparison of 6 MV and 18 MV photons for IMRT treatment of lung cancer. *Radiother Oncol* 2007; **82**: 63–69.
12. Rana SB. Dose prediction accuracy of anisotropic analytical algorithm and pencil beam convolution algorithm beyond high density heterogeneity interface. *South Asian J Cancer* 2013; **2**: 26-30.
13. Robinson D. Inhomogeneity correction and the analytic anisotropic algorithm. *J Appl Clin Med Phys 2008*; **9**: 112-122.
14. Rana S, Rogers K. Dosimetric evaluation of Acuros XB dose calculation algorithm with measurements in predicting doses beyond different air gap thickness for smaller and larger field sizes. *J Med Phys* 2013; **38**: 9-14.
15. Bush K, Gagne IM, Zavgorodni S, Ansbacher W, Beckham W. Dosimetric validation of Acuros XB with Monte Carlo methods for photon dose calculations. *Med Phys* 2011; **38**: 2208-2221.
16. Han T, Mourtada F, Kisling K, Mikell J, Followill D, Howell R. Experimental validation of deterministic Acuros XB algorithm for IMRT and VMAT dose calculations with the Radiological Physics Center's head and neck phantom. *Med Phys* 2012; **39**: 2193-2202.
17. Rana S, Rogers K, Lee T, Reed D, Biggs C. Verification and dosimetric impact of Acuros XB algorithm for stereotactic body radiation therapy (SBRT) and RapidArc planning for non-small-cell lung cancer (NSCLC) patients. *Int J Med Phys Clin Eng Radiat Oncol* 2013; **2**: 6-14.

 ISSN 2330-4049

International Journal of Cancer Therapy and Oncology
www.ijcto.org

Urological management (medical and surgical) of BK-virus associated haemorrhagic cystitis in children following haematopoietic stem cell transplantation

Nikhil Vasdev[1,3*], Angela Davidson[1], Christian Harkensee[2], Mary Slatter[2], Andrew R Gennery[2], Ian E Willetts[3], Andrew C Thorpe[1]

[1]*Departmentof Urology, Freeman Hospital, Newcastle upon Tyne, UK*
[2]*Supra-regional Children's Bone Marrow Transplant Unit (CBMTU), Newcastle General Hospital, Newcastle upon Tyne, UK*
[3]*Department of Paediatric Urology, Royal Victoria Infirmary, Newcastle upon Tyne, UK*

Received August 19, 2013; Revised September 06, 2013; Accepted September 07, 2013; Published Online September 09, 2013

Original Article

Abstract

Aim: Haemorrhagic cystitis (HC) is uncommon and in its severe form potentially life threatening complication of Haematopoietic stem cell transplantation (HSCT) in children. We present our single centre experience in the urological management of this clinically challenging condition. **Patients and Methods**: Fourteen patients were diagnosed with BK-Virus HC in our centre. The mean age at diagnosis was 8.8 years (range, 3.2-18.4 years). The mean number of days post-BMT until onset of HC was 20.8 (range, 1 – 51). While all patients tested urine positive for BKV at the clinical onset of HC, only four patients had viral quantification, with viral loads ranging from 97,000 to >1 billion/ml. 8 patients had clinical HC. Ten patients experienced acute GVHD (grade I: 6 patients, grade II: 3 patients, grade 4: 1 patient). **Results:** Four patients received medical management for their HC. Treatments included hyperhydration, MESNA, blood and platelet transfusion, premarin and oxybutynin (Table 6). Two patients received both medical and surgical management which included cystoscopy with clot evacuation, bladder irrigation and supra-pubic catheter insertion. One patient received exclusive surgical management. Seven patients were treated conservatively. **Conclusion**: There is limited available evidence for other potential therapeutic strategies highlighting the need for more research into the pathophysiology of HSCT-associated HC. Commonly used interventions with possible clinical benefit (e.g. cidofovir, ciprofloxacin) still require to be evaluated in multi-centre, high-quality studies. Potential future preventative and therapeutic options, such as modulation of conditioning, immunosuppression and engraftment, new antiviral and anti-inflammatory and less nephrotoxic agents need to be assessed.

Keywords: Haemorrhagic Cystitis; Haemopoitic Stem Cell Transplant; Urological Management; Patient Outcome

Introduction

A significant number of children undergo haematopoietic stem cell transplantation (HSCT) for a range of indications each year. There are various side effects and complications well understood, many of which occur secondary to immunosuppression. Haemorrhagic cystitis (HC) is characterised by haemorrhagic inflammation of bladder mucosa which results in painful micturition associated with haematuria. The clinical course of HC following HSCT can vary from from mild and brief (Grade I) to severe, prolonged and life-threatening (Grade IV).[1, 2]

Patients who develop HC following HSCT the onset have either an early or late onset presentation. Early onset occurs within days of transplantation and is associated with associated with conditioning regimen (chemotherapy or irradiation). The late-onset form occurs post-engraftment and is associated with the reactivation of urotropic viruses, principally BK virus, Adenovirus and CMV.[3] In current literature, numerous conditioning regimens have been used which in-

***Corresponding author:** Mr. Nikhil Vasdev, FRCS (Urology), Senior Specialist Registrar, Department of Urology, Freeman Hospital, Newcastle upon Tyne, United Kingdom; Phone: +44 (0) 1912336161; Fax: +44 (0) 1912137127.
Email: nikhilvasdev@doctors.org.uk

Cite this article as:
Vasdev N, Davidson A, Harkensee C, Slatter M, Gennery A, Willetts I, Thorpe A. Urological management (medical and surgical) of BK-virus associated haemorrhagic cystitis in children following haematopoietic stem cell transplantation. Int J Cancer Ther Oncol 2013; 1(1):01013. DOI: 10.14319/ijcto.0101.3

ISSN 2330-4049

clude of the initial use of less toxic conditioning regimens, uroprotective antitoxic agents (e.g. MESNA)[4] or hyperhydration/forced dieresis regimens.[5]

A common theory for the onset of HC following HSCT indicates the role of BK virus reactivation during the time of maximal post-transplant immune suppression in the pathogenesis of late-onset HC.[6] We present our single centre experience in the urological (medical and surgical) management of these patients with this clinically challenging and difficult clinical diagnosis to manage.

Methods and Materials

The aim of this case series was to investigate the cases of all children who underwent HSCT and developed BK-virus HC as a complication, over a 6 year period (2004-2009) at Newcastle General Hospital (NGH). Those who developed BK-virus positive HC following HSCT (n=14) were identified. Notes for all eligible children were sourced and data retrieved on a number of variables: diagnosis necessitating HSCT, date of HSCT, conditioning regimen, donor (whether related and nature of relationship or unrelated), HLA match, Adenovirus and CMV status both pre- and post-HSCT, Graft versus Host Disease (GvHD) prophylaxis, number of days post-HSCT of onset of GvHD, grade of maximal GvHD, treatment of GvHD, number of days post-HSCT of onset of HC, grade of HC, serial BK viral loads in both urine and serum, surgical treatment of HC, medical treatment of HC, serial CD45RA+ counts and eventual outcome. Data was presented on an excel spreadsheet prior to analysis.

Indications for haematopoietic stem cell transplantation (HSCT)

Fourteen patients in total, ten boys and four girls, with a mean age of 8.8 years underwent BMT on our unit between 2004 and 2009 and subsequently developed HC. There were a range of indications. Four had chronic granulomatous disease and two had complex autoimmune disease. The remaining nine patients presented with one of the following: combined immune deficiency, familial haemophagocyticlymphohistocytosis, idiopathic aplastic anaemia, IPEX like complex autoimmune disease, previous Wiskott Aldrich syndrome with chronic EBV, severe congenital neutropenia (HAX1 gene defect), severe periodic syndrome, T-cell acute lymphoblastic lymphoma (Table 1).

Conditioning

Ten different conditioning regimens were used in our patients, almost all of them myeloablative (Table 2). Five received busulfan, cyclophosphamide and campath. One received each of the following: cyclophosphamide only; busulfan and cyclophosphamide; campath, fludarabine and cyclophosphamide; campath, fludarabine and melphalen; campath, fludarabine and treosulphan; cyclophosphamide, rituximab and busulfan; melphalan, fludarabine and campath; rabbit ATG, busulfan and cyclophosphamide; treosulfan and cyclophosphamide.

TABLE 1: Indications for haematopoietic stem cell transplantation (HSCT)

Diagnosis	Number of Patients	% ofSeries
Chronic granulomatous disease	4	26.8
Complex autoimmune disease	2	13.3
Combined immune deficiency	1	6.7
Familial haemophagocyticlymphohistocytosis	1	6.7
Idiopathic aplastic anaemia	1	6.7
IPEX like complex autoimmune disease	1	6.7
Previous Wiskott Aldrich syndrome with chronic EBV	1	6.7
Severe congenital neutropenia (HAX1 gene defect)	1	6.7
Severe periodic syndrome	1	6.7
T-cell acute lymphoblastic lymphoma	1	6.7

TABLE 2: Conditioning regimen

Conditioning Regimen	Number of Patients	% ofSeries
Busulfan, cyclophosphamide and campath	5	33.5
Cyclophosphamide	1	6.7
Busulfan and cyclophosphamide	1	6.7
Campath, fludarabine and cyclophosphamide	1	6.7
Campath, fludarabine and melphalan	1	6.7
Campath, fludarabine and treosulphan	1	6.7
Cyclophosphamide, rituximab and busulfan	1	6.7
Melphalan, fludarabine and campath	1	6.7
Rabbit ATG, busulfan and cyclophosphamide	1	6.7
Treosulfan and cyclophosphamide	1	6.7

Donor Match

HLA matching was defined as 10/10 match (excluding HLA-DP), where HLA class I was largely low resolution and HLA class II high resolution typed. Except for one HSCT (9/10 match – HLA-A mismatched, unrelated donor) all were 10/10 HLA matched (Table 3).

TABLE 3: Donor Match

Donor Match	Number of Patients	% of Series
Unrelated donor (9/10 match)	1	6.7
Fully matched sibling donor	4	26.8
Fully matched unrelated donor	8	53.6
Fully matched maternal donor	1	6.7

 ISSN 2330-4049

CMV Status

Ten patients tested negative for CMV both pre and post BMT. Two patients tested negative for CMV pre-BMT and positive for CMV post-BMT. Two patients tested positive for CMV pre-BMT and negative for CMV post-BMT. Two patients had post-transplant adenovirus infection (Table 4).

TABLE 4: CMV Status

CMV Status Pre- and Post- BMT	Number of Patients	% of Series
Negative pre and post	10	67
Negative pre, positive post	2	13.3
Positive pre, negative post	2	13.3

Results

The mean age at diagnosis was 8.8 years (range 3.2-18.4 years). The mean number of days post-BMT until onset of HC was 20.8 (range 1 – 51). While all patients tested urine positive for BKV at the clinical onset of HC, only four patients had viral quantification, with viral loads ranging from 97,000 to >1 billion/ml. 8 patients had clinical HC (Table 5). Ten patients experienced acute GVHD (grade I: 6 patients, grade II: 3 patients, grade 4: 1 patient).

TABLE 5: Grade of Hemorrhagic Cystitis

Grade of HC	No of patients
0	4 (BKV viruria only)
I	4
II	2
III	1
IV	3

Grade[6]	Grading System for HC
Grade I	Microscopic haematuria
Grade II	Marcoscopichaematuria
Grade III	Macroscopic haematuria with small clots
Grade IV	Gross haematuria with clots causing urinary tract obstruction requiring instrumentation for clot evacuation

Four patients received medical management for their HC. Treatments included hyperhydration, MESNA, blood and platelet transfusion, premarin and oxybutynin (Table 6). Two patients received both medical and surgical management which included cystoscopy with clot evacuation, bladder irrigation and supra-pubic catheter insertion. One patient received exclusive surgical management (Table 7). Seven patients were treated conservatively.

TABLE 6: Medical Management

Management Strategy	Number of Patients	% of Series
Conservative management	7	46.9
Hyperhydration	4	26.8
MESNA	3	20.1
Blood and/or platelet transfusion	2	13.3
Premarin and oxybutynin	1	6.7

Table 7: Surgical Management

Management Strategy	Number of Patients	% of Series
Cystoscopy and clot evacuation	2	13.3
Heparinised saline bladder irrigation	2	13.3
Supra-pubic catheter insertion	1	6.7

Outcome

Of the fourteen patients two died. One died from multi organ failure, sepsis, on the basis of chronic granulomatous disease, with BMT cited in part II of the death certificate. The other patient died from pulmonary haemorrhage, pneumonia, also with underlying chronic granulomatous disease, with BMT cited in part II of the death certificate. The remaining twelve children survived to discharge and in all cases but one the HC was self-limiting. Eleven went home symptom free and one continued to have occasional macroscopic haematuria on discharge (Table 8).

TABLE 8: Final patient outcome

	Number of Patients	% of Series
Full recovery	11	73.7
Died	2	13.3
Occassional macroscopic haematuria	1	6.7

Discussion

Post-engraftment HC tends to present within one month of neutrophil engraftment, resulting in variable disease severity and duration (one week to four months)[7] suggesting multiple contributing risk factors. A three-phase model for post-engraftment HC has been suggested: uroepithelial insult by chemotherapy and radiation providing a permissive environment for virus replication (phase 1), reactivation secondary to immunosuppression (phase 2), and attack of infected uroepithelial cells by donor lymphoid cells upon engraftment, resulting in tissue destruction (phase 3)[8]. HLA and immune response gene polymorphisms are also likely to play a role in viral immune responses, as has previously been demonstrated in BK-virus nephropath.[9, 10]

BK-virus

BK-virus is a member of the Polyomaviridae family and was first described in 1971. It was isolated in cell culture from the urine of an asymptomatic immunosuppressed patient.[11] Primary infection with BK-virus usually occurs in childhood and is generally asymptomatic. Thereafter, the virus lies latent in the host. BK-virus is urotheliotropic, affecting epithelia of renal calyces, renal pelvis, ureter and urinary bladder. The widespread frequency of BK-virus in children suggests common routes of transmission such as respiratory or faecalspread.[6] Post HSCT HC with BK-virus is widely believed to result from reactivation of latent virus, although new or reinfection has also been postulated.[9, 12-14] Urinary BK

 ISSN 2330-4049

viral load can be quantified by PCR and urinary BK viral load peaks have been found to correlate with subsequent development of HC.[8, 15-17] Urine BK viral loads of >9 x 10^6 copies/ml and blood BK viral load >1 x 10^3 copies/ml are predictive of HC in children, with a higher sensitivity for urine monitoring.[6]

Incidence of BK-virus associated HCis varied across different transplant populations, ranging from 3.6% to 20%, according to definition of HC used. A number of prospective and retrospective case series have investigated risk factors for the development of post-engraftment HC, including myeloablative conditioning,[18] unrelated donor transplants,[19-21] and Adenovirus and CMV infection.[22-25] Demographic risk factors include male sex,[23, 26] and age >10 years [27-30]. GvHD is a consistent risk factor in paediatric [26, 28, 31], mixed [21, 30, 34], and adult [20] study cohorts. Busulphan [21, 34] and cyclophosphamide[28, 35] conditioning which are important risk factors for pre-engraftment HC, seem also to increase risk of post-engraftment HC. Immunosuppressive therapies, including T-cell depletion, ATG, methotrexate, cyclosporin and tacrolimus all lead to a higher incidence of HC.[21, 28, 29, 36-38]

The management of paediatric patients with post-HSCT HC is difficult. The clinician is confronted with a condition that is potentially life threatening with significant associated morbidity. The recent toxic insult, profound immunosuppression and co-morbidities such as renal impairment severely restrict therapeutic options, however, a recent systematic review supports MESNA and hyperhydration as medical preventative measures and use of recombinant Factor VII in the emergency treatment of acute haemorrhage unresponsive to alternative interventions.[6]

Medical Urological Management

Hyperhydration with forced diuresis has been studied in the context of pre-engraftment HC caused by the toxic metabolites of cyclophosphamide or ifosfamide. The uroprotective effect of 2-mercaptoethane sodium (MESNA) as a uroprotective antitoxic agent has been investigated as part of high-quality chemotherapy drug trials, and also with regards to efficacy, tolerability and safety compared with hyperhydration[5, 39] or prophylactic bladder irrigation.[40] Results are equivocal, with only one trial reporting an advantage of MESNA over forced diuresis/hyperhydration.[4] MESNA and hyperhydration appear to be equally effective in preventing HC, although current studies do not distinguish between early and late onset HC, therefore the protective impact on post-engraftment, BK-virus associated HC cannot clearly be determined.[6]

Recombinant activated Factor VII (rFVII) has a haemostatic effect leading to formation of thrombin and a haemostatic plug. rFVII was investigated in a randomised, placebo-controlled clinical trial.[41] This study enrolled 100 patients aged >12 years with bleeding complications between days 2-180 post-HSCT, 26 of whom had HC. rFVII was given in 3 different doses (40, 80 and 160 μg/kg) as seven single administrations over a 36 hour period, and compared with placebo. Overall, a reduction of the bleeding score at endpoint (38h after first administration) was observed for 80 μg/kg, but not for 160 μg/kg. Six thromboembolic events, including two deaths, were attributed to the study medication. A different dose regimen was used in a prospective case series on patients with HC after high-dose chemotherapy.[42] Seven adult patients received initial doses of 80 μg/kg, followed by two further administrations of 120 μg/kg at 3-hour intervals if bleeding persisted. Four patients had a complete, and a further two had partial short lasting responses although bleeding recurred to baseline within hours. Two further small case series report doses of 100 and 400 μg/kg [43] and 90 and 270 μg/kg [44] to be effective in HC. As a standard rFVII dose of 90 μg/kg costs around £4000 in the UK, treatments according to the above study protocols would cost between £12,000 (for three doses) and £28,000 (for seven doses),[45] thereby limiting its use to the most severe of cases.

The evidence for other medical interventions commonly used, and considered 'conventional' – systemic cidofovir, oestrogen, hyperbaric oxygen therapy, bladder instillation with alum, formalin or prostaglandins – have been reported to have a weak evidence base, are potentially highly toxic, or both.[6]

Hyperhydration was employed for three of our patients (21%) with grades II, III and IV HC. MESNA was used for one patient (7%) with grade II HC, and blood and platelet transfusion, premarin and oxybutynin was employed for another patient who also required surgical intervention with bladder irrigation.

Surgical Urological Management

Grade III or IV HC with blood clots often requires surgical intervention. Catheterisation with cystoscopic clot extraction may become necessary, and consideration should be given to continuous bladder irrigation with normal saline for prevention of clots and bladder tamponade, if required.[6]

HC can occasionally present so severe that it not only fails to respond to conservative measures, but also puts a patient's life at risk due to uncontrollable haemorrhage or renal failure secondary to complete urinary tract obstruction. Current case literature indicates cystectomy as the final step in the management of severe medically refractory HC.[46] Whether a radical or subtotal cystectomy should be performed depends largely on the policy of the unit. Preservation of the bladder neck has been recommended in children because severe HC is improved by cystotomy, temporary urinary diversion and bladder packing.[47] Currently, subtotal cystectomy with urethra and bladder neck preservation, allowing subsequent reconstructive continent urological surgery is the preferred option although experience is limited.[6]

 ISSN 2330-4049

Other surgical management options including use of fibrin glue, selective embolization, and intravesical hydrostatic pressure have been reported to have a weak evidence base or are associated with unacceptable risks.[6]

Catheterisation and bladder irrigation was only required for two patients (14%) in the current case series population and clot extraction for one patient (7%), indicating that the study unit is adhering to current guidelines in managing post-HSCT HC conservatively where possible, reserving invasive, surgical treatment options only in cases of grade IV HC refractive to simple treatment options.

Conclusion

Current guidance on management of post-HSCT HC advocates the following [6]:

- Prevention by addressing known risk factors early, employing the best possible donor-recipient matching, using the least toxic conditioning regimen with MESNA/hyperhydration, tight monitoring of viral titres and prompt treatment of re-activation in the peri-transplant period, GvHD prevention and tightly monitored immunosuppression.
- Optimal supportive treatment of manifest HC, with a conservative approach wherever possible and accompanying further management if required: ensuring appropriate hydration and maintenance of renal function, haematological homoeostasis (preserving high platelet counts, appropriate red cell counts and levels of clotting factors), pain relief, catheterisation with cystoscopic clot extraction and continuous bladder irrigation with normal saline for prevention of clots and bladder tamponade, if necessary.
- Early and close collaboration between medical and surgical teams in the management of these patients to coordinate and optimise timing of necessary interventions.
- As post-engraftment HC is by nature a transient condition that resolves with immune reconstitution, the goal is for a conservative approach avoiding measures that may inflict long-term consequences on the patient. Given the low grades of recommendation, any further interventions would have to be considered on an individual basis for a given clinical scenario, carefully balancing benefits and risks.

There is limited available evidence for other potential therapeutic strategies highlighting the need for more research into the pathophysiology of HSCT-associated HC. Commonly used interventions with possible clinical benefit (e.g. cidofovir, ciprofloxacin) still require to be evaluated in multi-centre, high-quality studies. Potential future preventative and therapeutic options, such as modulation of conditioning, immunosuppression and engraftment, new antiviral and anti-inflammatory and less nephrotoxic agents need to be assessed.[6]

Conflict of interest

The authors declare that they have no conflicts of interest. The authors alone are responsible for the content and writing of the paper.

References

1. Bedi A, Miller CB, Hanson JL, Goodman S, Ambinder RF, Charache P, Arthur RR, Jones RJ. Association of BK virus with failure of prophylaxis against hemorrhagic cystitis following bone marrow transplantation. *J Clin Oncol* 1995; **13**: 1103-9.
2. Iwamoto S, Azuma E, Hori H, Hirayama M, Kobayashi M, Komada Y, Nishimori H, Miyahara M. BK virus-associated fatal renal failure following late-onset hemorrhagic cystitis in an unrelated bone marrow transplantation. *Pediatr Hematol Oncol* 2002; **19**: 255-61.
3. Leung AY, Mak R, Lie AK, Yuen KY, Cheng VC, Liang R, Kwong YL. Clinicopathological features and risk factors of clinically overt haemorrhagic cystitis complicating bone marrow transplantation. *Bone Marrow Transplant* 2002; **29**: 509-13.
4. Hows JM, Mehta A, Ward L, Woods K, Perez R, Gordon MY, Gordon-Smith EC. Comparison of mesna with forced diuresis to prevent cyclophosphamide induced haemorrhagic cystitis in marrow transplantation: a prospective randomised study. *Br J Cancer* 1984; **50**: 753-6.
5. Shepherd JD, Pringle LE, Barnett MJ, Klingemann HG, Reece DE, Phillips GL.Mesna versus hyperhydration for the prevention of cyclophosphamide-induced hemorrhagic cystitis in bone marrow transplantation. *J Clin Oncol* 1991; **9**: 2016-20.
6. Harkensee C, Vasdev N, Gennery AR, Willetts IE, Taylor C. Prevention and management of BK-virus associated haemorrhagic cystitis in children following haematopoietic stem cell transplantation--a systematic review and evidence-based guidance for clinical management. *Br J Haematol* 2008; **142**: 717-31.
7. McCarville MB, Hoffer FA, Gingrich JR, Jenkins JJ 3rd. Imaging findings of hemorrhagic cystitis in pediatric oncology patients. *Pediatr Radiol* 2000; **30**: 131-8.
8. Leung AY, Chan MT, Yuen KY, Cheng VC, Chan KH, Wong CL, Liang R, Lie AK, Kwong YL. Ciprofloxacin decreased polyoma BK virus load in patients who underwent allogeneic hematopoietic stem cell transplantation. *Clin Infect Dis* 2005; **40**: 528-37.
9. Bohl DL, Storch GA, Ryschkewitsch C, Gaudreault-Keener M, Schnitzler MA, Major EO, Brennan DC. Donor origin of BK virus in renal

 ISSN 2330-4049

transplantation and role of HLA C7 in susceptibility to sustained BK viremia. *Am J Transplant* 2005; **5**: 2213-21.
10. Ellis D, Shapiro R, Randhawa P, Barmada M, Ferrell R, Vats A. Cytokine gene polymorphisms and risk of BK virus nephropathy in renal transplantation. *Am J Transplant* 2004; **4**: 160-307 (Abstracts1-543).
11. Gardner SD, Field AM, Coleman DV, Hulme B. New human papovavirus (B.K.) isolated from urine after renal transplantation. *Lancet* 1971; **1**: 1253-7.
12. Bogdanovic G, Priftakis P, Taemmeraes B, Gustafsson A, Flaegstad T, Winiarski J, Dalianis T. Primary BK virus (BKV) infection due to possible BKV transmission during bone marrow transplantation is not the major cause of hemorrhagic cystitis in transplanted children. *Pediatr Transplant* 1998; **2**: 288-93.
13. Dolei A, Pietropaolo V, Gomes E, Di Taranto C, Zicchedu M, Spanu MA, Lavorino C, Manca M, Degener AM. Polyomavirus persistence in ymphocytes: prevalence in lymphocytes from blood donors and healthy personnel of a blood transfusion centre. *J Gen Virol* 2000; **81**:1967-73.
14. Leung AY, Chan M, Kwong YL. Genotyping of the noncoding control region of BK virus in patients with haemorrhagic cystitis after allogeneic haematopoietic stem cell transplantation. *Bone Marrow Transplant* 2005; **35**: 531-2.
15. Azzi A, Cesaro S, Laszlo D, Zakrzewska K, Ciappi S, De Santis R, Fanci R,Pesavento G, Calore E, Bosi A. Human polyomavirus BK (BKV) load and haemorrhagic cystitis in bone marrow transplantation patients. *J Clin Virol* 1999; **14**: 79-86.
16. Bogdanovic G, Priftakis P, Giraud G, Kuzniar M, Ferraldeschi R, Kokhaei P, Mellstedt H, Remberger M, Ljungman P, Winiarski J, Dalianis T. Association between a high BK virus load in urine samples of patients with graft-versus-host disease and development of hemorrhagic cystitis after hematopoietic stem cell transplantation. *J Clin Microbiol* 2004; **42**: 5394-6.
17. Leung AY, Suen CK, Lie AK, Liang RH, Yuen KY, Kwong YL. Quantification of polyoma BK viruria in hemorrhagic cystitis complicating bone marrow transplantation. *Blood* 2001; **98**: 1971-8.
18. Giraud G, Bogdanovic G, Priftakis P, Remberger M, Svahn BM, Barkholt L, Ringden O, Winiarski J, Ljungman P, Dalianis T. The incidence of hemorrhagic cystitis and BK-viruria in allogeneic hematopoietic stem cell recipients according to intensity of the conditioning regimen. *Haematologica* 2006; **91**: 401-4. Erratum in: *Haematologica* 2009; **94**: 1630.
19. Bogdanovic G, Priftakis P, Giraud G, Dalianis T. A related donor and reduced intensity conditioning reduces the risk of development of BK virus-positive haemorrhagic cystitis in allogeneic haematopoetic stem cell-transplanted patients. *Anticancer Res* 2006; **26**: 1311-8.
20. Chakrabarti S, Osman H, Collingham K, Milligan DW. Polyoma viruria following T-cell-depleted allogeneic transplants using Campath-1H: incidence and outcome in relation to graft manipulation, donor type and conditioning. *Bone Marrow Transplant* 2003; **31**: 379-86.
21. Trotman J, Nivison-Smith I, Dodds A. Haemorrhagic cystitis: incidence and risk factors in a transplant population using hyperhydration. *Bone Marrow Transplant* 1999; **23**: 797-801.
22. Akiyama H, Kurosu T, Sakashita C, Inoue T, Mori Si, Ohashi K, Tanikawa S, Sakamaki H, Onozawa Y, Chen Q, Zheng H, Kitamura T. Adenovirus is a key pathogen in hemorrhagic cystitis associated with bone marrow transplantation. *Clin Infect Dis* 2001; **32**: 1325-30.
23. Asano Y, Kanda Y, Ogawa N, Sakata-Yanagimoto M, Nakagawa M, Kawazu M, Goyama S, Kandabashi K, Izutsu K, Imai Y, Hangaishi A, Kurokawa M, Tsujino S, Ogawa S, Aoki K, Chiba S, Motokura T, Hirai H. Male predominance among Japanese adult patients with late-onset hemorrhagic cystitis after hematopoietic stem cell transplantation. *Bone Marrow Transplant* 2003; **32**: 1175-9.
24. Tomonari A, Takahashi S, Ooi J, Fukuno K, Taka-sugi K, Tsukada N, Konuma T, Ohno N, Uchimaru K, Iseki T, Tojo A, Asano S. Hemorrhagic cystitis in adults after unrelated cord blood transplantation: a single-institution experience in Japan. *Int J Hema-tol* 2006; **84**: 268-71.
25. Yamamoto R, Kusumi E, Kami M, Yuji K, Hamaki T, Saito A, Murasgihe N, Hori A, Kim SW, Makimoto A, Ueyama J, Tanosaki R, Miyakoshi S, Mori S, Morinaga S, Heike Y, Taniguchi S, Masuo S, Takaue Y, Mutou Y. Late hemorrhagic cystitis after reduced-intensity hematopoietic stem cell transplantation (RIST). *Bone Marrow Transplant* 2003; **32**: 1089-95.
26. Hale GA, Rochester RJ, Heslop HE, Krance RA, Gingrich JR, Benaim E, Horwitz EM, Cunningham JM, Tong X, Srivastava DK, Leung WH, Woodard P, Bowman LC, Handgretinger R. Hemorrhagic cystitis after allogeneic bone marrow transplantation in children: clinical characteristics and outcome. *Biol Blood Marrow Transplant* 2003; **9**: 698-705.
27. Cesaro S, Brugiolo A, Faraci M, Uderzo C, Rondelli R, Favre C, Zecca M, Garetto G, Dini G, Pillon M, Messina C, Zanesco L, Pession A, Locatelli F. Incidence and treatment of hemorrhagic cystitis in children given hematopoietic stem cell transplantation: a survey from the Italian association of pediatric hematology oncology-bone marrow transplantation group. *Bone Marrow Transplant* 2003; **32**: 925-31.

 ISSN 2330-4049

28. Cheuk DK, Lee TL, Chiang AK, Ha SY, Lau YL, Chan GC. Risk factors and treatment of hemorrhagic cystitis in children who underwent hematopoietic stem cell transplantation. *Transpl Int* 2007; **20**: 73-81.
29. Kondo M, Kojima S, Kato K, Matsuyama T. Late-onset hemorrhagic cystitis after hematopoietic stem cell transplantation in children. *Bone Marrow Transplant* 1998; **22**: 995-8.
30. Seber A, Shu XO, Defor T, Sencer S, Ramsay N. Risk factors for severe hemorrhagic cystitis following BMT. *Bone Marrow Transplant* 1999; **23**: 35-40.
31. Russell SJ, Vowels MR, Vale T. Haemorrhagic cystitis in paediatric bone marrow transplant patients: an association with infective agents, GVHD and prior cyclophosphamide. *Bone Marrow Transplant* 1994; **13**: 533-9.
32. El-Zimaity M, Saliba R, Chan K, Shahjahan M, Carrasco A, Khorshid O, Caldera H, Couriel D, Giralt S, Khouri I, Ippoliti C, Champlin R, de Lima M. Hemorrhagic cystitis after allogeneic hematopoietic stem cell transplantation: donor type matters. *Blood* 2004; **103**: 4674-80.
33. Hassan Z, Remberger M, Svenberg P, Elbander M, Omazic B, Mattsson J, Conrad R, Svahn BM, Ahlgren A, Sairafi D, Aschan J, Le Blanc K, Barkholt L, Ringdén O. Hemorrhagic cystitis: a retrospective single-center survey. *Clin Transplant* 2007; **21**: 659-67.
34. Brugieres L, Hartmann O, Travagli JP, Benhamou E, Pico JL, Valteau D, Kalifa C, Patte C, Flamant F, Lemerle J. Hemorrhagic cystitis following high-dose chemotherapy and bone marrow transplantation in children with malignancies: incidence, clinical course, and outcome. *J Clin Oncol* 1989; **7**: 194-9.
35. Agha I, Brennan DC. BK virus and immunosuppressive agents. *Adv Exp Med Biol* 2006; **577**: 174-84.
36. Brennan DC, Agha I, Bohl DL, Schnitzler MA, Hardinger KL, Lockwood M, Torrence S, Schuessler R, Roby T, Gaudreault-Keener M, Storch GA. Incidence of BK with tacrolimus versus cyclosporine and impact of preemptive immunosuppression reduction. *Am J Transplant* 2005; **5**: 582-94. Erratum in*: Am J Transplant* 2005; **5**: 839.
37. Childs R, Sanchez C, Engler H, Preuss J, Rosenfeld S, Dunbar C, van Rhee F, Plante M, Phang S, Barrett AJ. High incidence of adeno- and polyomavirus-induced hemorrhagic cystitis in bone marrow allotransplantation for hematological malignancy following T cell depletion and cyclosporine. *Bone Marrow Transplant* 1998; **22**: 889-93.
38. Wu C, Randhawa P, McCauley J. Transplantation: polyomavirus nephropathy and the risk of specific immunosuppression regimens. *Scientific World Journal* 2006; **28**: 512-28.
39. Ballen KK, Becker P, Levebvre K, Emmons R, Lee K, Levy W, Stewart FM, Quesenberry P, Lowry P. Safety and cost of hyperhydration for the prevention of hemorrhagic cystitis in bone marrow transplant recipients. *Oncology* 1999; **57**: 287-92.
40. Vose JM, Reed EC, Pippert GC, Anderson JR, Bierman PJ, Kessinger A, Spinolo J, Armitage JO. Mesna compared with continuous bladder irrigation as uroprotection during high-dose chemotherapy and transplantation: a randomized trial. *J Clin Oncol* 1993; **11**: 1306-10.
41. Pihusch M, Bacigalupo A, Szer J, von Depka Prondzinski M, Gaspar-Blaudschun B, Hyveled L, Brenner B; F7BMT-1360 Trial Investigators. Recombinant activated factor VII in treatment of bleeding complications following hematopoietic stem cell transplantation. *J Thromb Haemost* 2005; **3**: 1935-44.
42. Ashrani AA, Gabriel DA, Gajewski JL, Jacobs DR Jr, Weisdorf DJ, Key NS. Pilot study to test the efficacy and safety of activated recombinant factor VII (NovoSeven) in the treatment of refractory hemorrhagic cystitis following high-dose chemotherapy. *Bone Marrow Transplant* 2006; **38**: 825-8.
43. Karimi M, Zakerinia M, Khojasteh HN, Ramzi M, Ahmad E. Successful treatment of cyclophosphamide induced intractable hemorrhagic cystitis with recombinant FVIIa (NovoSeven) after allogenic bone marrow transplantation. *J Thromb Haemost* 2004; **2**: 1853-5.
44. Blatt J, Gold SH, Wiley JM, Monahan PE, Cooper HC, Harvey D. Off-label use of recombinant factor VIIa in patients following bone marrow transplantation. *Bone Marrow Transplant* 2001; **28**: 405-7.
45. BNF, British National Formulary for Children. BMJ Publishing Group Ltd. 2006.
46. Garderet L, Bittencourt H, Sebe P, Kaliski A, Claisse JP, Espérou H, Ribaud P, Estrade V, Gluckman E, Gattegno B. Cystectomy for severe hemorrhagic cystitis in allogeneic stem cell transplant recipients. *Transplantation* 2000; **70**: 1807-11.
47. Andriole GL, Yuan JJ, Catalona WJ. Cystotomy, temporary urinary diversion and bladder packing in the management of severe cyclophosphamide-induced hemorrhagic cystitis. *J Urol* 1990; **143**: 1006-7.

 ISSN 2330-4049

International Journal of Cancer Therapy and Oncology
www.ijcto.org

Dose prediction accuracy of collapsed cone convolution superposition algorithm in a multi-layer inhomogenous phantom

Stephen Oyewale

Department of Radiation Oncology, Cancer Centers of Southwest Oklahoma, Lawton, Oklahoma, USA.

Received September 01, 2013; Revised September 17, 2013; Accepted September 18, 2013; Published Online September 18, 2013

Original Article

Abstract

Purpose: Dose prediction accuracy of dose calculation algorithms is important in external beam radiation therapy. This study investigated the effect of air gaps on depth dose calculations computed by collapsed cone convolution superposition (CCCS) algorithm. **Methods**: A computed tomography (CT) scan of inhomogenous phantom (30 × 30 × 30 cm^3) containing rectangular solid-water blocks and two 5 cm air gaps was used for central axis dose calculations computed by CCCS in Pinnacle treatment planning system. Depth dose measurements were taken using a cylindrical ionization chamber for identical beam parameters and monitor units as in the depth dose computations. The calculated and the measured percent depth dose (PDDs) were then compared. The data presented in this study included 6 MV photon beam and field sizes of 3 × 3 cm^2, 5 × 5 cm^2, 10 × 10 cm^2, and 15 × 15 cm^2. **Results:** The results of CCCS were within ±1.4% in the first water medium. However, upon traversing the first air gap and re-entering the water medium, in comparison to the measurements, the CCCS under-predicted the dose, with difference ranged from -1.6% to -3.3% for 3 × 3 cm^2, from -2.4% to -4.2% for 5 × 5 cm^2, from -2.4% to -6.7% for 10 × 10 cm^2, and from -1.6% to -6.3% for 15 × 15 cm^2. After the second air gap, the CCCS continued to under-predict the dose, and the difference ranged from -3.2% to -3.9% for 3× 3cm^2, from -2.4% to -5.6% for 5 × 5 cm^2, from -2.3% to -6.0% for 10 × 10 cm^2, and from -1.5% to -5.6% for 15 × 15 cm^2. **Conclusion**: The CCCS under-predicted the dose in water medium after the photon beam traversed the air gap. Special attention must be given during the patient set-up since large air gap between the patient body and immobilization devices may lead to unacceptable dose prediction errors.

Keywords: Collapsed Cone Convolution Superposition; Heterogeneity Correction; PDD; Pinnacle; Dose Calculation

Introduction

The significant advances in external beam radiation therapy (EBRT) such as beam delivery capabilities have improved the dose conformity and distributions.[1] The intensity modulation radiation therapy (IMRT) is an example of EBRT that combines several intensity modulated beams leading to the construction of conformal dose distributions.[2, 3] Most recently, a novel radiation technique called volumetric intensity modulated arc therapy (VMAT) was introduced.[3, 4] The VMAT systems can deliver a highly conformal radiation dose to the target by allowing the simultaneous variation of gantry rotation speed, dose rate and positions of multiple-leaf collimators (MLC). [3, 4]

Several authors have conducted the evaluation of dose calculation algorithms for external beam radiation therapy.[5-16] Rana *et al.*[16] investigated the dose prediction accuracy of Acuros XB algorithm and anisotropic analytical algorithm (AAA) for different field sizes and air gap thicknesses. The results from that study[16] revealed that dose predictions errors up to 3.8% for Acuros XB and up to 10.9% for AAA could occur during radiation treatment. Furthermore, the study by Rana *et al.*[16] demonstrated the limitation of dose calculation algorithms when treating a smaller size of tumor, especially when larger air gaps are created by immobilization devices. The motivation of our study was to further explore the dose

Corresponding author: Stephen Oyewale; Department of Radiation Oncology, Cancer Centers of Southwest Oklahoma, Lawton, Oklahoma, USA. Email: steve.oyewale@gmail.com

Cite this article as:
Oyewale S. Dose prediction accuracy of collapsed cone convolution superposition algorithm in a multi-layer inhomogenous phantom. Int J Cancer Ther Oncol 2013; 1(1):01016. **DOI**: 10.14319/ijcto.0101.6

A part of this research was presented at 52nd annual meeting of American Association of Physicists in Medicine (AAPM), which was held from August 4-8, 2013 in Indianapolis, Indiana, USA.

ISSN 2330-4049

prediction accuracy of different dose calculation algorithm called collapsed cone convolution superposition (CCCS) algorithm employed in ADAC Pinnacle³ 3D treatment planning system v. 9.0 (Philips Healthcare, Andover, MA). In this study, we used the similar methodology described by Rana *et al.*[16], but we investigated using two air gaps between two solid-water materials. The evaluation of CCCS was done by comparing the percent depth dose (PDD) calculated by CCCS with the measured PDD.

Methods and Materials

This study utilized a 6 Megavoltage (MV) X-ray beam from ElektaSynergy 1981 linear accelerator (Elekta AB, Stockholm). For all dose computations and measurements, the source to surface distance (SSD) was kept at 100 cm.

Collapsed Cone Convolution Superposition Algorithm

The CCCS superposition model uses an algorithm in which dose is computed from first principles, thereby accounting for patient heterogeneity and other modifiers.[17] This is done by modeling the energy fluence of the beam exiting the gantry head, computation of the total energy released per unit mass (TERMA) in the tissue volume, superposing the TERMA with an energy kernel, and accounting for electron contamination which is then added to the photon dose.[17-19] A detailed description on CCCS in provided elsewhere.[19]

Percent Depth Dose Calculation and Measurement

An inhomogeneous phantom (30 × 30 cm², 30 cm deep) composed of rectangular solid-water blocks and two 5 cm air gaps [Figure 1] was manufactured and scanned using Siemens Somatom Sensation Open CT (Siemens Medical Solutions USA, Inc., Malvern, PA).

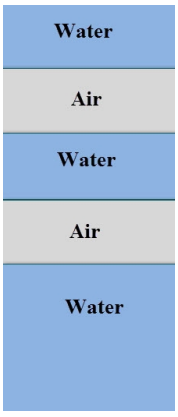

FIG. 1: Schematic diagram of an inhomogeneous phantom. The bottom or fifth layer (water medium) was 10 cm in thickness, whereas other four layers were each 5 cm in thickness.

The CT data set of phantom was transferred to the Pinnacle TPS from which a 3D structure set was created. The central axis depth dose calculations were then performed using CCCS for open field sizes 3 × 3 cm², 5 × 5 cm², 10 × 10 cm², and 15 × 15 cm², and for 100 monitor units (MUs). The dose calculation grid size was set to 4 mm.

At selected depths in the water medium of inhomogeneous phantom, measurements were performed using cylidnrical ionization chamber (PTW TN30013, 0.6 cm³ sensitive volume) for identical beam parameters and same number of MUs as in the depth dose calculations. The measurements at each depth were repeated three times. The calculated and measured depth doses were then normalized to the dose obtained at the depth of 1.7cm. The difference (Δ) between percent depth dose (PDD) computed by CCCS and the measured PDD was calculated by using Equation 1.

$$\Delta(PDD_d) = \frac{CCCS - MEAS}{MEAS} \times 100 \qquad \textbf{Eq. 1}$$

where, PDD_d = percent depth dose at depth, d; CCCS = collapsed cone convolution superposition; MEAS = measurement.

Results

The measured PDDs and calculated PDDs are presented in Figure 2 for field sizes 3 × 3 cm², 5 × 5 cm², 10 × 10 cm², and 15 × 15 cm².

First Water Medium

In the first water medium, the CCCS predicted the PDD within ±1.4% of measured PDD. The highest dose prediction error (up to -1.4%) was obtained for the smallest test field size.

Second Water Medium

In the second water medium (i.e., after the first air gap), the CCCS under-predicted the PDD at all depths for all four test field sizes. Specifically, dose prediction errors ranged from -1.6% to -3.3% for 3 × 3 cm², from -2.4% to -4.2% for 5 × 5 cm², from -2.4% to -6.7% for 10 × 10 cm², and from -1.6% to -6.3% for 15 × 15 cm².

Third Water Medium

In the third water medium, the CCCS continued to under-predict the PDDs at all depths for all test field sizes. Specifically, dose prediction errors ranged from -3.2% to -3.9% for 3 × 3 cm², from -2.4% to -5.6% for 5 × 5 cm², from -2.3% to -6.0% for 10 × 10 cm², and from -1.5% to -5.6% for 15 × 15 cm².

ISSN 2330-4049

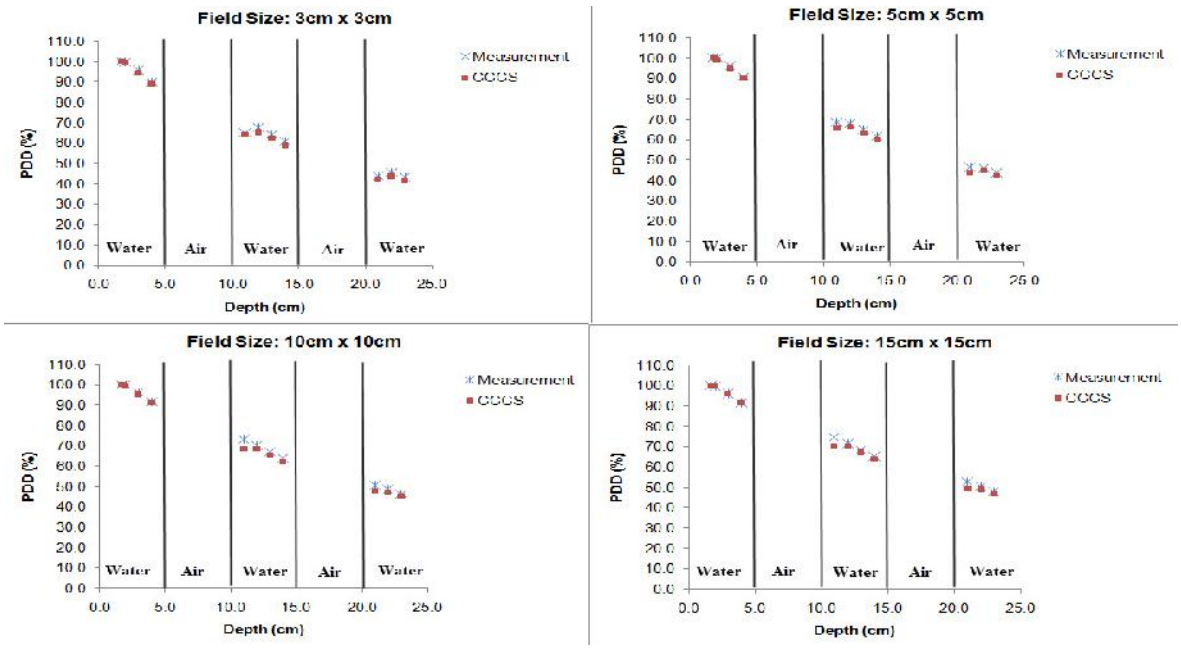

FIG. 2: Calculated and measured PDD for field sizes 3 × 3, 5 × 5, 10 × 10, and 15 × 15 cm^2 in inhomogeneous phantom. The first (top), second, third, fourth, and fifth (bottom) layers represent solid-water (5cm), air gap (5cm), solid-water (5cm), air gap (5cm) and solid-water (10cm) media, respectively, in the phantom. The measurements were done at SSD of 100 cm using 6 MV photon beam for 100 MUs, and all dose calculations and measurements were normalized to the reading obtained at depth of maximum dose (d_{max} = 1.7 cm). Abbreviations: PDD = Percent Depth Dose, CCCS = Collapsed Cone Convolution Superposition

Discussion

In this study, dose calculation accuracy of CCCS has been evaluated by comparing the calculated and measured PDD at multiple depths in an inhomogeneous slab phantom containing two air gaps. Although the CCCS had good agreement with the measurement in the first water medium, the results showed the limitation of CCCS in predicting doses in second water medium (i.e., after the first air gap) as well as in the third water medium (i.e., after the second air gap). As the photon beam traverses the air gap, loss of lateral scatter increases within the air gap, and this causes decreased scatter dose contribution to the points along the central beam axis. Furthermore, media of different density can cause the electronic disequilibrium at and near their heterogeneity interface.[5] Thus, dose discrepancies seen in the water media after the air gaps may be due to improper beam modeling within CCCS.

In this study, dose prediction accuracy of CCCS was investigated using low-density medium only. However, in real clinical situations, photon beams may also pass through the high-density tissues/materials before reaching the target. Future work involves the dosimetric evaluation of CCCS in inhomogeneous phantom that is composed of high- and low density materials such as bone and lung tissues. The limitation of CCCS must be further investigated in different clinical scenarios in order to avoid the dose overestimation or underestimation when CCCS is used for dose computations in external beam radiation therapy planning.

Conclusion

The results of this study showed that the CCCS under-predicted the depth doses in the water medium after the photon beam traversed the air gaps. Special attention must be given during the patient set-up since large air gap between the patient body and immobilization devices may lead to unacceptable dose prediction errors.

Conflict of interest

The authors declare that they have no conflicts of interest. The authors alone are responsible for the content and writing of the paper.

References

1. Webb S. Intensity-modulated radiation therapy. Bristol: Institute of Physics Publishing 2000.

 ISSN 2330-4049

2. Guerrero Urbano MT, Nutting CM. Clinical use of intensity-modulated radiotherapy: part I. *Br J Radiol* 2004; **77**:88–96.
3. Otto K. Volumetric modulated arc therapy: IMRT in a single gantry arc. *Med Phys* 2008; **35**: 310–317.
4. Teoh M, Clark CH, Wood K, Whitaker S, Nisbet A. Volumetric modulated arc therapy: A review of current literature and clinical use in practice. *Br J Radiol* 2011; **84**: 967–96.
5. Das IJ, Ding GX, Ahnesjö A. Small fields: Non-equilibrium radiation dosimetry. *Med Phys* 2008; **35**: 206–15.
6. Robinson D. Inhomogeneity correction and the analytic anisotropic algorithm. *J Appl Clin Med Phys* 2008; **9**:2786.
7. Ding W, Johnston P, Wong T, et al. Investigation of photon beam models in heterogeneous media of modern radiotherapy. *Australas Phys Eng Sci Med* 2004; **27**: 39–48.
8. Carrasco P, Jornet N, Duch M, et al. Comparison of dose calculation algorithms in phantoms with lung equivalent heterogeneities under conditions of lateral electronic disequilibrium. *Med Phys* 2004; **31**: 2899–2911.
9. Krieger T, Sauer OA. Monte Carlo- versus pencil-beam-/collapsed-cone-dose calculation in a heterogeneous multi-layer phantom. *Phys Med Biol* 2005; **50**:859-68.
10. Van Esch A, Tillikainen L, Pyykkonen, et al. Testing of the analytical anisotropic algorithm for photon dose calculation. *Med Phys* 2006; **33**: 4130-48.
11. Dobler B, Walter C, Knopf A, Fabri D, Loeschel R, Polednik M, Schneider F,Wenz F, Lohr F. Optimization of extracranial stereotactic radiation therapy of small lung lesions using accurate dose calculation algorithms. *Radiat Oncol* 2006; **1:45**.
12. Vanderstraeten B, Reynaert N, Paelinck L, Madani I, De Wagter C, De Gersem W, De Neve W, Thierens H. Accuracy of patient dose calculation for lung IMRT: A comparison of Monte Carlo, convolution/superposition, and pencil beam computations. *Med Phys* 2006; **33**:3149-58.
13. Gray A, Oliver LD, Johnston PN. The accuracy of the pencil beam convolution and anisotropic analytical algorithms in predicting the dose effects due to attenuation from immobilization devices and large air gaps. *Med Phys* 2009; **36**:3181-3191.
14. Rana S, Rogers K, Lee T, Reed D, Biggs C. Verification and Dosimetric Impact of Acuros XB Algorithm for Stereotactic Body Radiation Therapy (SBRT) and RapidArc Planning for Non-Small-Cell Lung Cancer (NSCLC) Patients. *Int J Med Phys Clin Eng Rad Onc* 2013; **2**: 6-14.
15. Han T, Mourtada F, Kisling K, Mikell J, Followill D, Howell R. Experimental validation of deterministic Acuros XB algorithm for IMRT and VMAT dose calculations with the Radiological Physics Center's head and neck phantom. *Med Phys* 2012; **39**: 2193-2202.
16. Rana S, Rogers K. Dosimetric evaluation of Acuros XB dose calculation algorithm with measurements in predicting doses beyond different air gap thickness for smaller and larger field sizes. *J Med Phys* 2013; **38**:9-14.
17. Ahnesjö A. Collapsed cone convolution of radiant energy for photon dose calculation in heterogeneous media. *Med Phys* 1989; **16**:577-92.
18. Mackie TR, Scrimger JW, Battista JJ. A convolution method of calculating dose for 15-MV X rays. *Med Phys* 1985; **12**:188-96.
19. McNutt T. Dose calculations: collapsed cone convolution superposition and delta pixel beam. 2002: Pinnacle White Paper No. 4535 983 02474.

 ISSN 2330-4049

International Journal of Cancer Therapy and Oncology
www.ijcto.org

Dosimetric study of SIB-IMRT versus SIB-3DCRT for breast cancer with breath-hold gated technique

Suresh Moorthy[1], Hamdi Sakr[1], Shubber Hasan[1], Jacob Samuel[1], Shaima Al-Janahi[1], Narayana Murthy[2]

[1]*Department of Oncology & Hematology, Salmaniya Medical Complex, Kingdom of Bahrain*
[2]*Department of Physics, Acharya Nagarjuna University, Guntur, India*

Received September 05, 2013; Revised October 02, 2013; Accepted October 08, 2013; Published Online October 10, 2013

Original Article

Abstract

Background and purpose: 3-dimensional conformal therapy (3DCRT) is widely employed radiation therapy technique for breast cancer, but there is still need to minimize the doses to organ at risk (OAR) using 3DCRT. A few clinical studies have discussed using intensity modulated radiation therapy (IMRT) to address this shortfall. Simultaneous integrated boost (SIB) has been used in head and neck and prostate cancer, and there is a growing interest in using SIB for breast cancer too. This study aimed to compare SIB-IMRT versus SIB-3DCRT for breast cancer patients. **Materials and Methods:** SIB-3DCRT treatment plans were created for 36 consecutive patients. Dose was prescribed as 45 Gy in 25 fractions to the planning target volume (PTV)-1 and 60 Gy in 25 fractions to PTV-2. Treatment plans were normalized to 95% of PTV volume receiving 95% of the prescription dose. The conformity index (CI), homogeneity index (HI), lung dose, heart dose, left anterior descending artery(LAD) dose, and low dose volume and integral dose of normal healthy tissue were recorded and analyzed. **Results:** With the use of IMRT technique, there was an improvement in CI (0.14) when compared to CI of 3DCRT (0.18; $p = 0.01$). However, there was no significant difference in the HI ($p = 0.45$). On average, the V_{20Gy} of ipsilateral lung was 37.9 % for 3DCRT and 22.4 % ($p < 0.01$) for IMRT, whereas the V_{20Gy} of total lung (ipsilateral + contralateral) was 21.8% for 3DCRT and 12.14 ($p < 0.01$) for IMRT. Similarly, average V_{40Gy} of heart was 7.5 % for 3DCRT and 2.13 % ($p = 0.01$) for IMRT. The LAD maximum dose to left side breast patients, on average, was 39.5 Gy for 3DCRT and 29.17 Gy ($p = 0.03$) for IMRT. The average number of monitor units was about 180 for 3DCRT and 1441 ($p < 0.01$) for IMRT. **Conclusion:** IMRT for breast cancer treatment is feasible. In comparison to 3DCRT, IMRT can reduce the maximum dose to the target volume, and dose to the OAR. However, 3DCRT technique is superior in terms of low dose volume, integral dose, and treatment time. With the use of breath-hold gated technique in IMRT, it can further improve the target coverage and reduction of doses to the heart, lung, and LAD. SIB technique could reduce the overall treatment duration by about one week.

Keywords: Intensity Modulated Radiation Therapy, Three Dimensional Conformal Radiotherapy, Simultaneous Integrated Boost, Breath-Hold, Technique, Breast Cancer

Introduction

Breast cancer is the most common malignancy in women. Radiotherapy is an integral part of breast cancer management either in breast conservation surgery (BCS) or in post mastectomy cases. Many prospective studies have shown that adjuvant radiotherapy improves local control and survival rate in breast cancer patients after surgery.[1] During earlier days of radiotherapy, opposed wedged fields with half beam block was considered as the standard radiation therapy technique. In the last decade, an introduction of linear accelerators has made 3-dimensional conformal radiotherapy (3DCRT) as a standard treatment technique, which can re-duce the doses to the lung, heart, and other critical structure doses in the breast cancer treatment. However, using 3DCRT, it is not always possible to achieve adequate normal tissue sparing, especially when treating left side chest wall patients. This is mainly due to overlying concave shape of

Corresponding author: Suresh Moorthy, M.Sc, M.Phil; Division of Radiation Oncology, Department of Oncology & Hematology, Salmaniya Medical Complex, MOH, Kingdom of Bahrain.
Email: nmsureshm@gmail.com

Cite this article as: Moorthy S, Sakr H, Hasan S, Samuel J, Al-Janahi S, Murthy N. Dosimetric study of SIB-IMRT versus SIB-3DCRT for breast cancer with breath-hold gated technique. Int J Cancer Ther Oncol 2013;1(1):010110.
DOI: 10.14319/ijcto.0101.10

 ISSN 2330-4049

the target, which can result more doses to adjacent structures such as heart and lung. Hong *et al.*[2] compared intensity modulated radiation therapy (IMRT) with 3D conformal tangential wedged beams, and showed the reduction of dose to the coronary arteries, contra lateral breast, ipsilateral lung, and surrounding soft tissues using IMRT. By modulating photon beam, it is possible to obtain concave and convex shape dose distributions with IMRT, and it has the ability to conform radiation dose to irregular target volumes sparing the underlying critical structures resulting in better tumor control probability (TCP) and reduced normal tissue complication probability (NTCP). The main purpose of this study was to further evaluate normal tissue sparing and dosimetric analysis of simultaneous integrated boost (SIB)-3DCRT and SIB-IMRT in breast patients, with focus on breath-hold gated technique.

Materials and Methods

In this retrospective treatment planning study, we used computed tomography (CT) data of 36 consecutive patients with breast cancer post lumpectomy (18 left sides and 18 right sides), and all patients were treated with respiratory gated technique for breast radiotherapy.

CT Simulation

All 36 patients were simulated using 4D CT scanner (Philips Medical Systems, Andover, MA, USA) with whole-body Vaclok (Civco Medical Solutions, Iowa, USA) immobilization system. Patients were positioned on a wide bore CT-SIM couch with the help of lasers, and both arms of the patient were raised above patient's head. Furthermore, radio opaque markers were placed during the immobilization procedure to guide the isocenter shift. For all the patients, CT scans images were obtained from mandible to upper abdomen area with intravenous contrast, and CT scans were obtained using slice thickness of 5 mm. Prior to CT simulation, patients were given training on breath-hold technique.

Target Delineation and Dose Prescription

After the CT simulation, the Digital Imaging and Communications in Medicine (DICOM) images were transferred to Eclipse treatment planning system (TPS) (version 10.0.34, Varian Medical Systems, Palo Alto, California, USA). Clinical target volume (CTV), planning target volume (PTV) and Organ at Risk (OAR) volumes were delineated on the axial CT slices. The lumpectomy gross tumor volume (L-GTV) was contoured using all available clinical and radiographic information including the excision cavity volume, architectural distortion, lumpectomy scar, seroma and/or extent of surgical clips.

CTV1 included the palpable breast tissue demarcated with radio opaque markers at CT simulation. The apparent CT glandular breast tissue visualized by CT, consensus definitions of anatomical borders, and the lumpectomy CTV from the RTOG breast cancer atlas. The breast CTV is limited anteriorly within 3 mm from the skin and posteriorly to the anterior surface of the pectoralis, serratous anterior muscle excluding chest wall. PTV was created by 3D expansion of CTV1 by 7 mm. CTV2 was created by 1 cm 3D expansion from L-GTV and was limited posteriorly at anterior surface of the pectoralis and antero-laterally 3 mm from skin. PTV2 was created by 7 mm 3D expansion of CTV2. The normal structures were contoured as ipsilateral lung, contra lateral lung, contra lateral breast, heart, left anterior descending (LAD) artery, spinal cord, esophagus, trachea, humerus head, and liver. Dose prescription was applied per International Commission on Radiological Units and Measurements (ICRU) 50 and 62.[3, 4] Specifically, dose was prescribed as 45 Gy in 25 fractions (1.8Gy/fraction) to the PTV-1 and 60 Gy in 25 fractions (2.4Gy/fraction) to PTV-2.

Treatment planning

For treatment planning, 6 mega-voltage (MV) X-rays from Clinac 600CD linear accelerator (Varian Medical Systems, Palo Alto, California, USA) integrated with 120 leaves millennium multi-leaf collimator (MLC) was used. For the dynamic IMRT plans, 7 non-coplanar beams were used to achieve the minimum criteria of 95% of the volume received 95% of the prescribed dose. The treatment fields were almost evenly spaced within an arc of 180^0 on the side of the tumor. Gantry angles ranged from 330^0 to 150^0 (clockwise) for the left side tumors and from 50^0 to 210^0 (counterclockwise) for the right side tumors. In Eclipse TPS, the IMRT plans were created with inverse plan optimization, and the algorithm used was Dose Volume Optimizer (version 10.0.28). For the dose calculation, pencil beam convolution (PBC) algorithm (version 10.0.28) was used, and leaf motions were calculated with leaf motion calculator (LMC) algorithm (version 10.0.28). Heterogeneity correction was done using modified Batho method in the Eclipse. For plan optimization, OAR dose constraints were given as ipsilateral lung $V_{20} < 30$ %, heart V_{30}, V_{40}, and mean dose as low as possible, contra-lateral breast mean dose less than 5 Gy, and spinal cord maximum point dose less than 40 Gy. For the 3DCRT plans, 4 to 6 non-coplanar beams were used to produce adequate dose coverage for the PTV. Critical organs were shielded using MLC without compromising PTV coverage. Beam weights were adjusted until the optimum coverage and acceptable hot spots were achieved. Additionally, field-in-field was created to reduce hotspot equal to or lower than 110% as well as to improve the target coverage and homogenous dose distribution in the PTV.

Plan evaluation

Dose-Volume Histograms (DVH) was used to analyze the volume receiving 20 Gy, 30 Gy and 40 Gy, mean, maximum and minimum doses. The target dose uniformity and conformity were calculated and evaluated. Different scoring indices were given by various authors.[5-7] In this study, we have followed indices defined by ICRU 83.[8]

 ISSN 2330-4049

The conformity index (CI) as defined in ICRU 83 is

$$CI_{ref} = \frac{\text{Volume of PTV covered by the reference dose}}{\text{Volume of PTV}} \quad \text{Eq. 1}$$

CI = 1.0 is ideal value

The Homogeneity Index (HI) as defined in ICRU 83 is

$$HI = \frac{D_{2\%} - D_{98\%}}{D_{50\%}} \quad \text{Eq. 2}$$

Where, $D_{2\%}$, $D_{98\%}$, $D_{50\%}$ is dose received by 2%, 98%, 50% volume. HI = 0 (Zero) is ideal value. Also, to illustrate the low dose volume effect, V_{5Gy} volume and integral dose were calculated for normal healthy tissue.

Integral Dose = Mean Dose (Gy) × Volume (Cm^3) Eq. 3

Statistical Analysis

Statistical Analysis was performed using the Wilcoxon Signed Rank test. This matched pair t test was applied to determine the statistical difference between the dose–volume data for IMRT versus 3DCRT. The values are reported in ranges. The reported p value is two tailed, and p values of < 0.05 are considered statistically significant.

Results and Discussion

Dose volume histograms of the normal tissues of both the plans (IMRT and 3DCRT) are presented in **Table 1.** The normalized target coverage of both treatment methods is presented in **Table 2 and Table 4**. The PTV mean dose for 3DCRT is 47.10 Gy compared to 45.88 Gy ($p < 0.01$) with IMRT. The dose distribution in axial sections is shown in **Figures 1 and 2**. These axial sections clearly show that concave PTV coverage and exclusion of LAD during optimization by IMRT. Also, previous studies have reported lower doses to the ipsilateral lung, contra lateral lung, contra lateral breast, heart, and LAD doses using IMRT technique.[10, 11]

3D conformal plans using asymmetric jaw and field-in-field technique provides better coverage than a conventional physical wedged –half beam blocked or physical wedged-asymmetric fields. Furthermore, physical wedge has limitation in field width and lengths. With 3DCRT, the hot spots occurred in superficial skin surface, but IMRT exhibited better control in shifting the hot spots, with a possibility of keeping dose to the skin equal to or less than the prescription dose.

Dose homogeneity and conformity

The use of equally spaced gantry angles improved homogeneity and conformity indices as well as reduced the volume of critical normal tissues such as the heart and ipsilateral lung receiving a high dose as shown by Hong *et al.* [2]. In this study, we used equally spaced beam angles for both the IMRT and 3DCRT plans, and the average target maximum dose was lower with IMRT; however, it was not statistically significant. Although the mean breast volume in our study was 1221 cc, which is relatively higher compared to the literature [12], we were able to demonstrate optimized coverage and reduced dose to the critical organs.

The inverse-planning IMRT further reduced hotspots mainly due to beam modulation during optimization compared to 3DCRT, where beam modulation is not available. Previous planning studies[13,14] with multiple fields showed the PTV-95% coverage values ranging from 90% to 97 %, whereas all our optimized plans had the PTV-95% coverage values of >95% of prescription dose. With the use of IMRT technique, our data showed that there is a consistent improvement in conformity index from 0.18 for 3DCRT to 0.15 for IMRT (p=0.01). However, there was no significant difference (p = 0.45) when HI of 3DCRT was compared to that of IMRT.

TABLE 1: Comparison of normal tissue dose volume parameters for Respiratory Gated IMRT and 3DCRT breast cancer patients (Statistics based on Wilcoxon Signed Rank Test). The values are averaged over 36 analyzed patients.

Organ	Parameter	SIB-3DCRT	SIB-IMRT
Ipsilateral lung	V_{20Gy} (%)	37.9	22.4
	V_{30Gy} (%)	32.24	16.08
	Mean (Gy)	20.29	16.51
Heart	V_{40Gy} (%)	7.5	2.13
Both Lung	V_{20Gy} (%)	21.8	12.14
LAD	Max. Dose (Gy)	39.5	29.17

TABLE 2: Comparison of planning target volume (PTV1) coverage parameter for Respiratory Gated IMRT and 3DCRT breast cancer patients (Statistics based on Wilcoxon Signed Rank Test). The values are averaged over 36 analyzed patients.

PTV 1 Parameter	SIB-3DCRT	SIB-IMRT	p
Minimum Dose (Gy)	24.07	32.03	<0.01
Maximum Dose (Gy)	51.97	59.68	<0.01
Coverage (%)	96.8	98.22	<0.01
Conformity Index	0.18	0.14	0.01
Homogeneity Index	1.03	1.01	0.45
Mean Dose (Gy)	47.1	45.88	<0.01
Mod Dose (Gy)	49.12	48.92	0.32
Median Dose (Gy)	50.5	48.8	<0.01
Stnd. Deviation(Gy)	6.35	4.17	<0.01
V_{50Gy} (%)	48.69	29.83	<0.01
V_{55Gy} (%)	30.7	11.29	<0.01

 ISSN 2330-4049

FIG. 1: Axial slice showing dose distribution in 3DCRT plan. The 3DCRT was unable to exclude LAD while covering the concave target, and increased dose to the heart and lung was noticed.

FIG. 2: Axial slice showing dose distribution in IMRT plan. The IMRT was able to exclude LAD while covering the concave target, and decreased dose to the heart and lung was noticed.

TABLE 3: Comparison of MU, ID and V5 parameter for Respiratory Gated IMRT and 3DCRT breast cancer patients (Statistics based on Wilcoxon Signed Rank Test). The values are averaged over 36 analyzed patients.

Parameter	SIB-3DCRT	SIB-IMRT	p
Monitor Units	180	1441	<0.01
Integral Dose (Gy-Cm^3)	145210	197428	<0.01
V_{5Gy} (%)	18.89	30.61	<0.01

TABLE 4: Comparison of planning target volume (PTV2) coverage parameter for Respiratory Gated IMRT and 3DCRT breast cancer patients (Statistics based on Wilcoxon Signed Rank Test). The values are averaged over 36 analyzed patients.

PTV 2 Parameter	SIB-3DCRT	SIB-IMRT	p
Minimum Dose (Gy)	56.41	53.9	<0.01
Maximum Dose (Gy)	64.9	64.01	<0.01
Coverage (%)	98.3	99.77	0.13
Conformity Index	0.12	0.08	0.01
Homogeneity Index	1.02	1.01	0.11
Mean Dose (Gy)	61.1	61.72	0.13
Mod Dose (Gy)	61.17	62.13	<0.01
Median Dose (Gy)	61.99	62.45	<0.01
Stnd. Deviation(Gy)	1.5	1.21	0.01

TABLE 5: Comparison of Non-Gated IMRT with respiratory Gated IMRT (mean) breast cancer patients (Statistics based on Wilcoxon Signed Rank Test). The values are averaged over 36 analyzed patients.

Parameters	Non-Gated SIB-IMRT	Gated SIB-IMRT	p
LAD-Maximum Dose	35.62 Gy	29.17 Gy	<0.01
Heart -V_{30Gy}	9.27 %	5.91 %	<0.01
Ipsilateral Lung-V_{20Gy}	30.2 %	22.4 %	0.03
PTV -95% of prescription	96.81%	98.22 %	<0.01

In patients with breast cancer, it is intended that the irradiated heart volume be minimized to the greatest possible degree without compromising the target coverage. The risk of pericardial events is probably related to both dose and volume of radiation. The incidences of pericardial disease decrease with the use of sub cranial blocking the major ventricles at 30 Gy. Stewart *et al.* [15] concluded that the dose should be limited to 60 Gy for less than 25% of cardiac volume and 45 Gy for more than 65% of cardiac volume.

In patients with breast cancer, it is intended that the irradiated heart volume be minimized to the greatest possible degree without compromising the target coverage. The risk of pericardial events is probably related to both dose and volume of radiation. The incidences of pericardial disease decrease with the use of sub cranial blocking the major ventricles at 30 Gy. Stewart *et al.* [15] concluded that the dose should be limited to 60 Gy for less than 25% of cardiac volume and 45 Gy for more than 65% of cardiac volume.

In our study the heart V_{40Gy} was significantly lower in IMRT than in 3DCRT ($p < 0.01$), especially for left sided breast cancer patients, with mean heart $V_{40\,Gy}$ of 7.5% for 3DCRT versus IMRT as 2.13% ($p = 0.01$). Gagliardi *et al.*[16] reported that CAD risk was much reduced at doses less than 30 Gy. Mean values of V_{30Gy} were <5% for IMRT compared with studies[17] reporting V_{30Gy} values in the range of 2% to 5%. Increased cardiac mortality risk associated with left side breast patients in the long term was reported by multiple authors.[16, 18, 19] The advancement in treatment techniques such as IMRT has enabled to reduce cardiac exposure, and steady decline of radiation risk is being noticed.[20] Furthermore, Boivin *et al.*[21] noted that the anteriorly placed coronary arteries were more often affected by radiation therapy (compared with the circumflex artery). In our study, mean LAD maximum dose was 39.5 Gy for 3DCRT and 29.17 Gy for IMRT ($p = 0.03$).

Lung dose

The occurrence of radiation pneumonitis (RP) is related to the ipsilateral lung volume irradiated.[22] In our study, the ipsilateral lung V_{20Gy} for IMRT (22.4%) is significantly less than that for 3DCRT (37.9%; $p < 0.01$). Ipsilateral lung mean dose was also higher in 3DCRT (20.29 Gy) compared to the one in IMRT (16.51Gy) ($p < 0.01$). Both the lung V_{20Gy} and

ISSN 2330-4049

mean dose were significantly lower in IMRT than in 3DCRT ($p < 0.01$). Contra lateral lung V_{5Gy} and mean dose of both the plans showed no significant differences. The mean lung doses (MLD) of both lung were higher compared to the report from Marks *et al.*[23], and this may be due to larger breast volumes in our study. Since there is no absolute safe MLD below which there is no pneumonitis, the clinically acceptable risk of RP depends on the risk-benefit ratio of the individual patient selection basis.

Secondary malignancy

The IMRT plans contributed a modestly higher dose to adjacent healthy soft tissues. In our study, the mean V_{5Gy} volume for 3DCRT was much lower than that of IMRT. The main concern with healthy tissue dose increases of this magnitude is an increased risk of late second malignancy.[24, 25] Some investigators suggest that IMRT might increase the incidence of secondary cancer from 1% in conventional planning to 1.75% in IMRT planning for patient's surviving 10 years.[24]

Furthermore, the treatment Monitor Unit (MU) was significantly higher in IMRT technique. The monitor unit for IMRT is 6-8 times more than 3DCRT is a concern.[24, 26, 27] This in turn shows that the integral dose would be higher. Pirzkall *et al.* [28] studied that the integral dose for IMRT was higher than conventional treatment. Similar observation was made in our study as integral dose for IMRT was 22% higher than that for 3DCRT. This higher integral dose was probably due to increased number of beams used in IMRT than in 3D CRT, thus involving larger volume of healthy tissue during IMRT plan optimization. Modulation of beams also increases the treatment time during treatment delivery. Furthermore, the leakage and scatter dose to non-target tissue of the patients will be proportional to the number of monitor units used. Few studies [13, 29] have found to have increased low dose volumes with increasing beam angles.

High integral dose attributed to second malignancy, which is likely to be of greatest concern in younger women and in patients with a low risk for systemic relapse that are likely to live for many years after the diagnosis of breast cancer.[27] There have been reports[24] suggesting that adjuvant radiation therapy for breast cancer may increase the risk of lung cancer and angiosarcoma. The risk of sarcoma in the treated volume is likely to be similar with IMRT or standard techniques, but it is possible that second primary lung cancers might be increased by IMRT, especially if the woman is a smoker.[27] Therefore, individual assessment of treatment volume goals and longevity of patients with and without radiation therapy is necessary in order to balance the short to medium-term benefits of reducing the volume of critical structures, especially heart and lung, receiving higher radiation dose.

Respiratory gating

Organ motion during the IMRT treatment has been accounted for using real-time position management (RPM; Varian Medical System, Palo Alto, California, USA). The RPM system supports automatic on and off triggering of radiation beam during the treatment. The marker position approximates identical and in-phase alignment of breast and marker motion. Due to breathing motion, the PTV may move outside the external contour as defined on the planning CT and result in a geographic miss of the target. Although the geometric uncertainties and intra fraction movement are taken into account on PTV margin, but the breast is a superficial organ and often the CTV will extend to the skin surface. In these cases, the restriction of the PTV to 3 mm from the skin surface will not provide an adequate margin for intra-fraction breathing motion.[29-33] The main concern would be the CTV being under-dosed. In order to use gating, the PTV motion must be in phase with the breathing cycle or must at least be able to be predicted from the breathing cycle using technology such as RPM. Conformal blocking and breath-hold techniques can essentially eliminate the heart from the primary beams. Historically, whole heart doses up to 30 Gy were reasonably well tolerated. [34-36]

Conclusion

IMRT for breast cancer treatment is feasible. In comparison to 3DCRT, IMRT reduced the maximum dose to the target volume, and dose to OAR was reduced too. However, 3DCRT technique was superior in terms of low dose volume of normal tissue, integral dose, and treatment time. Consequences of these low doses would have to be weighed against the benefits of reducing high doses on individual patient selection basis. With the use of breath-hold gated technique in IMRT, it can further improve the target coverage and reduction of doses to the heart, lung, and LAD. SIB technique could reduce the overall treatment duration by about one week.

Competing interests

The authors declare that they have no conflicts of interest. The authors alone are responsible for the content and writing of the paper.

References

1. Overgaard M, Nielsen HM, Overgaard J. Is the benefit of post mastectomy irradiation limited to patients with four or more positive nodes, as recommended in international consensus reports? A subgroup analysis of the DBCG 82 b & c randomized trials. *Radiother Oncol* 2007; **82**:247-253.
2. Hong L, Hunt M, Chui C, Spirou S, Forster K, Lee H, Yahalom J, Kutcher GJ, McCormick B. Intensity modulated tangential beam irradiation of the intact breast. *Int J Radiat Oncol Biol Phys* 1999; **44**:1155-64.

 ISSN 2330-4049

3. Prescribing, recording and reporting photon beam therapy. *International commission on Radiological Units and Measurements* (ICRU) Report # 50: *ICRU* 1993.
4. Prescribing, recording and reporting photon beam therapy. *International commission on Radiological Units and Measurements* (ICRU) Report # 62: ICRU 1997.
5. Baltas D, Kolotas C, Geramani K, Mould RF, Ioannidis G, Kekchidi M, Zamboglou N. A conformal index (COIN) to evaluate implant quality and dose specification in brachytherapy. *Int J Radiat Oncol Biol Phys* 1998; **40**: 515-24.
6. Knoos T, Kristensen I, Nilsson P. Volumetric and dosimetric evaluation of radiation treatment plans: Radiation Conformity Index. *Int J Radiat Oncol Biol Phys* 1998; **42**: 1169-76.
7. Paddick I. A simple scoring ratio to index the conformity of radiosurgical treatment plans. Technical note. *J Neurosurg* 2000; **93**:219-22.
8. Prescribing, recording and reporting photon beam therapy. *International commission on Radiological Units and Measurements* (ICRU) Report # 83: ICRU 2010.
9. Mohan R, Wu Q, Manning M, Schmidt-Ullrich R. Radiobiological considerations in the design of fractionation strategies for intensity-modulated radiation therapy of head and neck cancers. *Int J Radiat Oncol Biol Phys* 2000; **46**:619-630.
10. Zhou GX, Xu SP, Dai XK, et al. Clinical dosimetric study of three radiotherapy techniques for postoperative breast cancer: Helical Tomotherapy, IMRT, and 3D-CRT. *Technol Cancer Res Treat* 2011;**10**:15-23.
11. Selvaraj RN, Beriwal S, Pourarian RJ, et al. Clinical implementation of tangential field intensity modulated radiation therapy (IMRT) using sliding window technique and dosimetric comparison with 3D conformal therapy (3DCRT) in breast cancer. *Med Dosim* 2007; **32**:299-304.
12. Moody AM, Mayles WP, Bliss JM, et al. The influence of breast size on late radiation effects and association with radiotherapy dose inhomogeneity. *Radiother Oncol* 1994; **3**:106-112.
13. Chui CS, Hong L, Hunt M, McCormick B. A simplified intensity modulated radiation therapy technique for the breast. *Med Phys* 2002; **29**:522–529.
14. Donovan EM, Bleackley NJ, Evans PM, Reise SF, Yarnold JR. Dose-position and dose-volume histogram analysis of standard wedged and intensity modulated treatments in breast radiotherapy. *Br J Radiol* 2002; **75**:967–973.
15. Stewart JR, Fajardo LF, Gillette SM, Constine LS. Radiation injury to the heart. *Int J Radiat Oncol Biol Phys* 1995; **31:1205**-12.
16. Gagliardi G, Constine LS, Moiseenko V, et al. Radiation dose-volume effects in the heart. *Int J Radiat Oncol Biol Phys* 2010; **76**:S77-85.
17. Rongsriyam K, Rojpornpradit P, Lertbutsayanukul C, et al. Dosimetric study of inverse-planed intensity modulated, forward-planned intensity modulated and conventional tangential techniques in breast conserving radiotherapy. *J Med Assoc Thai* 2008; **91**:1571–1582.
18. Ragaz J, Olivotto IA, Spinelli JJ, et al. Locoregional radiation therapy in patients with high-risk breast cancer receiving adjuvant chemotherapy: 20-Year results of the British Columbia Randomized trial. *J Natl Cancer Inst* 2005; **97:116**–126.
19. Høst H, Brennhovd I, Loeb M. Postoperative radiotherapy in breast cancer - long term results from the Oslo study. *Int J Radiat Oncol Biol.Phys* 1986;**12**:727–732.
20. Giordano SH, Kuo Y, Freeman JL, et al. Risk of cardiac death after adjuvant radiotherapy for breast cancer. *J Natl Cancer Inst* 2005; **97:419**–424.
21. Boivin JF, Hutchison GB, Lubin JH, et al. Coronary artery disease mortality in patients treated for Hodgkin's disease. *Cancer* 1992; **69**:1241–1247.
22. Recht A, Ancukiewicz M, Alm El-Din MA, et al. Lung dose-volume parameters and the risk of pneumonitis for patients treated with accelerated partial-breast irradiation using three-dimensional conformal radiotherapy. *J Clin Oncol* 2009; **27**:3887-3893.
23. Marks LB, Bentzen SM, Deasy JO, et al. Radiation dose-volume effects in the lung. *Int J Radiat Oncol Biol Phys* 2010; **76**:S70-76.
24. Hall EJ, Wuu CS. Radiation-induced second cancers: The impact of 3D-CRT and IMRT. *Int J Radiat Oncol Biol Phys* 2003; **56**:83–88.
25. Gao X, Fisher SG, Emami B. Risk of second primary cancer in the contralateral breast in women treated for early-stage breastcancer: A population-based study. *Int J Radiat Oncol Biol Phys* 2003; **56**:1038–1045.
26. Jothybasu KS, Bahl A, Subramani V, et al. Static versus dynamic intensity-modulated radiotherapy: Profile of integral dose in carcinoma of the nasopharynx. *J Med Phys* 2009; **34**:66-72.
27. Followill D, Geis P, Boyer A. Estimates of whole-body dose equivalent produced by beam intensity modulated conformal therapy. *Int J Radiat Oncol Biol Phys* 1997; **38**:667-672.
28. Pirzkall A, Carol M, Lohr F, et al. Comparison of intensity-modulated radiotherapy with conventional conformal radiotherapy for complex-shaped tumors. *Int J Radiat Oncol Biol Phys* 2000; **48**:1371-1380.
29. Cho BCJ, Schwarz M, Mijnheer BJ, Bartelink H. Simplified intensity-modulated radiotherapy using pre-defined segments to reduce cardiac complica-

 ISSN 2330-4049

tions in left-sided breast cancer. *Radiother Oncol* 2004; **70:**231–41.
30. Pedersen AN, Korreman S, Nystrom H, *et al.* Breathing adapted radiotherapy of breast cancer: reduction of cardiac and pulmonary doses using voluntary inspiration breath-hold. *Radiother Oncol* 2004; **72**:53-60.
31. Kron T, Perera F, Lee C, Yu E. Evaluation of intra- and inter fraction motion in breast radiotherapy using electronic portal cine imaging. *Technol Cancer Res Treat* 2004; **3:**443-50.
32. Wong JW, Sharpe MB, Jaffray DA, et al. The use of active breathing control (ABC) to reduce margin for breathing motion. *Int J Radiat Oncol Biol Phys* 1999; **1**:911-9.
33. Jagsi R, Moran JM, Kessler ML, et al. Respiratory motion of the heart and positional reproducibility under active breathing control. *Int J Radiat Oncol Biol Phys* 2007; **68:**253-258.
34. Gagliardi G, Constine LS, Moiseenko V, Correa C, Pierce LJ, et al. Radiation dose-volume effects in the heart. *Int J Radiat Oncol Biol Phys* 2010; **76**: S77-85.
35. Giraud P, Djadi-Prat J, Morvan E, Morelle M, Remmonay R, Pourel N, Durdux C, Carrie C, Mornex F, Le Péchoux C, Bachaud JM, Boisselier P, Beckendorf V, Dendale R, Daveau C, Garcia R; les centres investigateurs du Stic. Dosimetric and clinical benefits of respiratory-gated radiotherapy for lung and breast cancers: results of the STIC 2003. *Cancer Radiother* 2012; **16:**272-81.
36. Stephen C, James R, Derek W, Lee S, Ivo AO. Respiratory Gating: Using Deep Inspiration Breath Hold Radiation Therapy to Treat Left Breast Cancer. *Journal of Medical Imaging and Radiation Sciences* 2008; **39**:192–197.

 ISSN 2330-4049

International Journal of Cancer Therapy and Oncology
www.ijcto.org

MicroRNAs as molecular markers in lung cancer

Javier Silva[1], Vanesa Garcia[1], Ana Lopez-Gonzalez[2], Mariano Provencio[1]

[1]*Medical Oncology Department, Hospital Universitario Puerta de Hierro, Majadahonda-Madrid, Spain*
[2]*Medical Oncology Department, Complejo Asistencial Universitario de León, Spain*

Received September 04, 2013; Revised October 04, 2013; Accepted October 07, 2013; Published Online October 10, 2013

Review Article

Abstract

Lung cancer is the most common cause of cancer death in the western world for both men and women. Lung cancer appears to be a perfect candidate for a screening program, since it is the number one cancer killer, it has a long preclinical phase, curative treatment for the minority of patients who are diagnosed early and a target population at risk (smokers) and it is also a major economic burden. The earliest approaches to identifying cancer markers were based on preliminary clinical or pathological observations, although molecular biology is a strong candidate for occupying a place among the set of methods. In search of markers, several alterations, such as mutations, loss of heterozygosity, microsatellite instability, DNA methylation, mitochondrial DNA mutations, viral DNA, modified expression of mRNA, miRNA and proteins, and structurally altered proteins have all been analysed. MicroRNAs (miRNA) are small RNA molecules, about 19-25 nucleotides long and encoded in genomes of plants, animals, fungi and viruses. It has been reported that miRNAs may have multiple functions in lung development and that aberrant expression of miRNAs could induce lung tumorigenesis. We review here the role of miRNAs in lung tumorigenesis and also as a novel type of biomarker.

Keywords: Lung Cancer, MicroRNA, Biomarker, Tumorigenesis

Introduction

Lung cancer is the most common cause of cancer death in the western world for both men and women.[1] Each year the number of lung cancer deaths is greater than the number of deaths from breast, prostate and colorectal cancer combined.[2] In 2007, estimates calculated 213,380 new cases of lung cancer and 160,390 deaths, accounting for 15% and 29%, respectively, of all cases of cancer.[2] Clinically, lung cancer can be divided into 2 groups: small cell lung cancer (SCLC) and non-small cell lung cancer (NSCLC), which often have different specific genetic alterations.[3] Approximately 75% of lung tumours are NSCLC, which includes squamous cell carcinoma, adenocarcinoma and large cell carcinoma.[1] SCLC is characterized by its rapid growth, early dissemination and chemosensitivity andradiosensitivity.[4]

Over 80% of lung cancers are attributable to cigarette smoking[5], with a risk directly proportional to consumption. Thus, cessation of smoking remains the single most important intervention for lung cancer prevention: recently some progress has been made by the introduction of smoking bans in public places throughout Europe. Although the exposure to tobacco carcinogens is known to be the main risk factor for lung cancer, only a minority of heavy smokers will develop this disease[6], suggesting environmental or genetic determinants in disease initiation and progression. Thus, inter-individual differences in carcinogen metabolism may play an essential role in the development of this environmental cancer.[7] In addition, with the increasing incidence of non-smoking-related lung cancers, particularly in women, the identification of high-risk groups among non-smokers will be an important challenge.[8]

Whereas screening the general population has been recommended for other common cancers, including breast, colorectal and possibly prostate cancer, no such recommendation currently exists for lung cancer.[9] Only between 10-16% of lung cancer patients survive more than 5 years.[2] The dismal

Corresponding author: Mariano Provencio, MD, PhD; Medical Oncology Department, Calle Manuel de Falla, 1 Majadahonda, Madrid 28222, Spain.
Email: mprovenciop@gmail.com

Cite this article as: Silva J, Garcia V, Lopez-Gonzalez A, Provencio M. MicroRNAs as molecular markers in lung cancer.Int J Cancer Ther Oncol 2013;1(1):010111. **DOI**: 10.14319/ijcto.0101.11

ISSN 2330-4049

prognosis of lung cancer is largely related to the fact that this tumour is generally diagnosed at a late stage. However, outcome is significantly better in patients diagnosed early, with the 5-year survival rate of stage 1 lung cancer at 60-70%.[10] Early detection of lung cancer could change disease outcome, although current diagnostic tools are either too costly or not sensitive enough to allow early detection.[11, 12] For all these reasons, it is essential to develop an effective screening regimen for this disease.

Lung cancer appears to be a perfect candidate for a screening program, since it is the number one cancer killer, it has a long preclinical phase, curative treatment for the minority of patients who are diagnosed early and a target population at risk (smokers) and it is also a major economic burden.

Molecular markers

The progression from pre-neoplasia to cancer is accompanied by the accumulation of genetic and epigenetic alterations. These lead to altered expression patterns and modifications in protein structure and function. The changes can be used as molecular tumour markers, being useful in: a) characterization of a predisposition or genetic susceptibility to suffering neoplasia; b) detection of cancer at early stages or pre-malignant phases; c) the evaluation of disease outcome; d) monitoring of disease progression; and e) determination of response to therapy, so favouring a better choice of therapy for each patient.

Currently, the diagnostic tools for lung carcinoma are: chest X-ray, computed tomography (CT), cytological analysis of sputum and bronchoalveolar lavage fluid, and spiral CT, among others. However, to develop more strategies, diagnosis, prognosis and treatment need to be improved. The goal of clinical and potential molecular markers is to develop a clinical screening test that would be useful and practical in clinical practice, complementing the use of imaging modalities such as spiral CT.

The earliest approaches to identifying cancer markers were based on preliminary clinical or pathological observations[13], although molecular biology is a strong candidate for occupying a place among the set of methods. In search of markers, several alterations, such as mutations, loss of heterozygosity, microsatellite instability, DNA methylation, mitochondrial DNA mutations, viral DNA, modified expression of mRNA, miRNA and proteins, and structurally altered proteins have all been analyzed. High-throughput screening approaches that analyze expression patterns of several genes and proteins have been used to search for cancer-associated molecules.[13] In lung carcinomas several alterations have been found, such as *KRAS* mutated in approximately 30% of cases[14], over-expression of *C-erbB2* (Her-2/neu) or *BCL2* in 25% of cases[14] and *DLC1* (deleted in lung cancer 1) altered in 27% of primary NSCLC.[15]

In clinical practice, there are several molecular tumour markers used for screening in some tumour types, such as serum carcino-embryonic antigen (CEA) in colorectal cancer[16] and prostate-specific antigen (PSA) in prostate cancer.[17] However, these markers are not very sensitive in premalignant or early stages or are not specific to malignancy. For most other types of cancer, such as early-stage lung cancer, there are no molecular markers available in clinical practice.

Although many effective cancer therapies have recently been developed, there are only a few molecular markers that are available at present for determining treatment response. For example, breast cancer cells that express high levels of the tyrosine receptor kinase are more likely to respond to trastuzumab.[18] In lung cancer, the ability to predict responses to chemotherapy or targeted agents is extremely limited and is based on tumour histology alone. Therefore, we are unable to identify *a priori* the right treatment regimen for each tumour. Appropriate molecular markers could predict response to specific treatments. An example is the use of epithelial growth factor tyrosine kinase inhibitors (EGFR-TKIs) in lung cancer.[19] Although more studies are necessary, it has been described that a series of mutations in EGFR makes tumours highly sensitive to this form of therapy. Thus, detection of these mutations could identify a group of patients who derive great benefit from EGFR-TKI therapy.[19] Another example is the use of molecular markers in relation to cisplatin treatment. Only a proportion of lung cancer patients will respond to this chemotherapy treatment, whose adverse side-effects are significant. Cisplatin needs to bind to DNA, creating platinum-DNA adducts, which can be repaired by nucleotide excision. Patients with completely resected NSCLC and ERCC1-negative tumours (enzyme with central role in DNA repair) appear to benefit from adjuvant cisplatin-based chemotherapy, whereas patients with ERCC1-positive tumours do not.[20]

microRNAs as molecular markers

MicroRNAs (miRNA) are small RNA molecules, about 19-25 nucleotides long and encoded in genomes of plants, animals, fungi and viruses.

miRNAs constitute a highly conserved class of naturally occurring non-coding single-stranded RNA molecules, which function as post-transcriptional negative gene regulators of complementary target mRNAs. Although they may differ in distinct organisms, the basic process involves a transcription of dsRNA that is processed into shorter units that mediate target recognition in a sequence-specific manner (Table 1).[21] It has been calculated that between 74% and 92% of the gene transcripts are probably under miRNA control.[22, 23]

 ISSN 2330-4049

TABLE 1:Main Studies that have investigated miRNA in lung cancer

Yanaihara *et al.* Cancer Cell. 2006
Lu *et al.* Proc Am Thorac Soc. 2008
Fabbri *et al.* Proc Natl Acad Sci. 2007
Inamura *et al.* Lung Cancer. 2007
Yu *et al.* Cancer Cell. 2008
Fagi F. Thorac Surg Clin. 2012
Rabinowits *et al.* Clin Lung Cancer. 2009
Hu *et al.* J Clin Oncol. 2010
Hennessey *et al.* PLoS One. 2012
Bianchi *et al.* E cancer medical science. 2012
Matsubara *et al.* Oncogene. 2007
Shen *et al.* Lab Invest. 2011
Rani *et al.* Cancer Biol. Ther. 2013
Xu *et al.* Clin Transl Oncol. 2013
Zhang *et al.* Med Oncol. 2013

miRNAs are specifically expressed or greatly enriched in a particular organ, implying an organ- or tissue-specific function. Furthermore, expression profiles of miRNAs in mice and human lung are very similar, indicating evolutionary conservation of miRNA expression.[24, 25] It has been reported that lung is one of the tissues with the most abundant expression of miRNA let-7.[26]

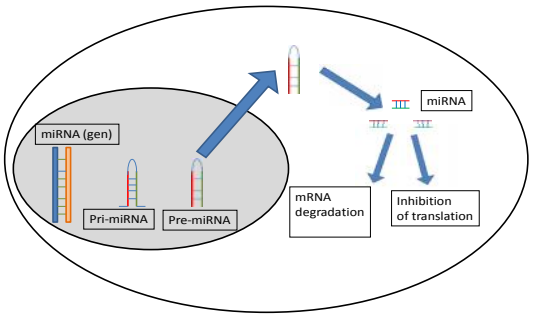

FIG. 1: miRNA function

There are several human diseases, such as spinal muscular atrophy, Parkinson's disease, fragile X mental retardation or DiGeorge syndrome, in which miRNAs or their processing might be involved.[27-29] Among human diseases, it is well-known that miRNAs are aberrantly expressed in numerous human cancers, including colon, breast, ovarian, prostate and lung cancer[30, 31] (Figure 1). Moreover, since a single miRNA may have as many as a few thousand target genes with different biological entities, the data obtained from miRNA profiling may provide information that can be used to classify more accurately the different cancer subtypes described to date. Besides regulating the expression of known oncogenes and tumour suppressors, miRNAs also act as oncogenes and tumour suppressors directly, which provides an apparent connection between the altered expression of miRNAs and cancer development. Thus, miRNA-expression profile of human tumours is closely associated with diagnosis, staging, progression, prognosis and response to treatment.[31-33]

In the case of lung cancer, it has been reported that miRNAs may have multiple functions in lung development and that aberrant expression of miRNAs could induce lung tumorigenesis.[34, 35] Moreover, as mentioned above, the different expression profiles of miRNAs between normal lung and lung cancer has led to their emergence as a novel type of biomarker. This may be helpful for lung cancer diagnosis and therapy using miRNAs as novel therapeutic targets.[36, 37]

The current diagnostic tools available for lung cancer often lack sensitivity and the ability to distinguish different lung cancer subtypes, such as NSCLC and SCLC or adenocarcinoma and squamous cell carcinoma.[38, 39] In this respect, the applicability of miRNA-based biomarkers may improve methodology for both sensitivity and specificity. Differently expressed miR-29 (a, b and c), miR-99b, miR-102, let-7a-2 and let-7f-1 have been used to discriminate histological types of lung carcinomas.[32, 40] As well as data strongly supporting the view that miRNAs work as biomarkers for differentiating lung cancer, the expression of miRNA signatures has been linked to the prognosis of lung cancer. Deregulated expression of the let-7 family has been frequently described in different analyses of miRNA expression signatures in lung cancer. The decrease in the let-7 family is associated with worse prognosis and shortened survival, which supports the view that it has a tumour suppression function.[41-43] Deregulated miRNA has been also related with lymph node metastasis and advanced clinical stage.[44]

Talking about EGFR-TKIs, we know that patients with activating EGFR mutations eventually develop resistance to this drugs. It is thought that a secondary mutation in the EGFR gene, such as T790M, or amplification of the MET proto-oncogene could be implicated. Recently, upregulated miR-214 has been related to acquired resistance to gefitinib, via PTEN/AKT signalling pathway.[45]

MicroRNAs in plasma from cancer patients

The presence in plasma or serum of circulating nucleic acids (DNA and RNA) released by tumour cells increases the possibility of detecting alterations associated with the tumour and could be used as a tumour marker. Furthermore, as circulating nucleic acids are a source of tumour information obtained through a non-invasive and rapid method, samples could be taken at different times during follow-up to identify residual disease and recurrence at asymptomatic stages.

MiRNAs originating in several tumour tissues enter circulation and can be detected in serum. The fact that plasma contains large amounts of stable miRNAs implies a great potential of serum miRNA profiling as the fingerprint for disease.[46] Regarding the release mechanism of nucleic acids from tumour cells to the bloodstream, we recently reported that a major fraction of these molecules detected in plasma of can-

 ISSN 2330-4049

cer patients are highly protected in tumour-specific microvesicle-like structures.[47] In other studies, cancer-specific miRNAs with high resistance to RNases and harsh conditions were identified in plasma or serum of cancer patients[46, 48-52], showing that the high stability conferred by its particle-associated features makes miRNA levels well suited for being tested as non-invasive cancer biomarkers in patient plasma samples. Moreover, other studies have suggested that miRNAs contained in tumour vesicles are functional and suppress target mRNAs for signal transduction components within recipient cells.[53]

Recently, our group as well as other research groups have analysed serum miRNA profiles of lung cancer patients to evaluate their potential use in predicting diagnosis and prognosis of disease.[46, 54, 55] Employing Solexa sequencing analysis, the Chen *et al.*[46] identified specific expression patterns of serum miRNAs for lung cancer in the Chinese population. They provided evidence that serum miRNAs contained fingerprints for different cancer types. Most differently expressed miRNAS in lung cancer included miR-205 and miR-206 that were previously involved in tumorigenic processes such as cell division and cell growth. Similarly, Lodes et al. focused their study on the evaluation of miRNA expression profiles in human serum for five types of human tumours, including lung cancer, using a pan-human microRNA high-density microarray. They found that these expression patterns could be used to distinguish between normal and cancer patient samples and, furthermore, that one millilitre of serum contained sufficient miRNAs to detect these expression patterns, without requiring amplification techniques. In a recent study, Hu's group analyzed the differences in levels of serum miRNAs between 30 NSCLC patients with longer survival and 30 patients with shorter survival. Using Solexa sequencing, they found 11 differently altered miRNAs between longer-survival and shorter-survival groups and, moreover, levels of 4 of them (miR-1, miR-30d, miR-486 and miR499) were significantly associated with overall survival.

Recently, a phase I//II biomarker study has been published, in which serum miRNA using PCR was examined from 30 NSCLC patients and 20 healthy controls. A combination of two differentially expressed miRNAs miR-15b and miR-27b was able to discriminate NSCLC from healthy controls.[56]

Combining serum mi-RNA detection and low-dose computed tomography (LD-CT) could be an interesting screening test. Real-time PCR was used to identify the profile of miRNAs extracted from the serum of asymptomatic LD-CT-detected lung adenocarcinoma and normal serum. A multivariate risk-predictor was developed based on 34 miRNA expression levels. When the predictor was tested on an independent cohort of patients with asymptomatic LD-CT detected lung cancer, it displayed an overall accuracy of 80% (sensitivity 71%, specificity 90%), and more important, the risk-predictor was able to distinguish between LD-CT-detected benign nodules and malignant disease.[57] We agree with the relevance of this last point, due to the relative high number of benign lung nodules detected by LD-CT screening.

Conclusion

miRNAs are frequently altered in many types of tumours, including lung carcinoma. Their expression patterns are associated with the classification and prognosis of these tumours. That miRNAs are stable in plasma from lung cancer patients supports their use as important clinical biomarkers[58, 59, 60] detectable in peripheral blood associated with tumour.

The fact that certain miRNAs have an oncogenic function while others have a role as tumour suppressors is especially relevant in terms of their applicability in anti-tumour therapies. Thus, oncogenic miRNAs would require therapies inhibiting their function, while those therapies for miRNAs with tumour suppressor ability should increase miRNA activity in cancer cells. There are some studies that analyze the potential of miRNA-based therapies in cancer.[61, 62]

In summary, the expression of miRNA signatures in plasma from lung cancer patients can be used as new markers, obtained by a non-invasive method, for disease diagnosis and prognosis. They have higher specificity and sensitivity than analyses used currently.

References

1. Risch A, Plass C. Lung cancer epigenetics and genetics. *Int J Cancer* 2008; **123**: 1-7.

2. Jemal A, Siegel R, Ward E, Hao Y, Xu J, Murray T, Thun MJ. Cancer statistics. *CA Cancer J Clin* 2008; **58**:71-96.

3. Girard L, Zöchbauer-Müller S, Virmani AK, Gazdar AF, Minna JD. Genome-wide allelotyping of lung cancer identifies new regions of allelic loss, differences between small cell lung cancer and on-small cell lung cancer, and loci clustering. *Cancer Res* 2000; **60**:4894-906.

4. Cooper S, Spiro SG. Small cell lung cancer: treatment review. *Respirology* 2006; **11**: 241-8.

5. Khuder SA. Effect of cigarette smoking on major histological types of lung cancer: a meta-analysis. *Lung Cancer* 2001; **31**:139-48.

6. Mattson ME, Pollack ES, Cullen JW. What are the odds that smoking will kill you? *Am J Public Health* 1987; **77**:425-31.

 ISSN 2330-4049

7. Schwartz AG, Prysak GM, Bock CH, Cote ML. The molecular epidemiology of lung cancer. *Carcinogenesis* 2007; **28**:507-18.

8. Wakelee HA, Chang ET, Gomez SL, Keegan TH, Feskanich D, Clarke CA, Holmberg L, Yong LC, Kolonel LN, Gould MK, West DW. Lung cancer incidence in never smokers. *J Clin Oncol* 2007; **25**:472-8.

9. Smith RA, Cokkinides V, Eyre HJ. Cancer screening in the United States, 2007: a review of current guidelines, practices, and prospects. *CA Cancer J Clin* 2007, **57**:90-104.

10. Spira A, Ettinger DS. Multidisciplinary management of lung cancer. *N Engl J Med* 2004; **350**:379-92.

11. International Early Lung Cancer Action Program Investigators, Henschke CI, Yankelevitz DF, Libby DM, Pasmantier MW, Smith JP, Miettinen OS. Survival of patients with stage I lung cancer detected on CT screening. *N Engl J Med* 2006; **355**:1763-71.

12. Markowitz SB, Miller A, Miller J, Manowitz A, Kieding S, Sider L, Morabia A. Ability of low-dose helical CT to distinguish between benign and malignant noncalcified lung nodules. *Chest* 2007; **131**:1028-34.

13. Sidransky D. Emerging molecular markers of cancer. *Nat Rev Cancer* 2002; **2**:210-9.

14. Salgia R, Skarin AT. Molecular abnormalities in lung cancer. *J Clin Oncol* 1998; **16**:1207-17.

15. Daigo Y, Nishiwaki T, Kawasoe T, Tamari M, Tsuchiya E, Nakamura Y. Molecular cloning of a candidate tumor suppressor gene, DLC1, from chromosome 3p21.3. *Cancer Res* 1999; **59**:1966-72.

16. Benson AB 3rd, Choti MA, Cohen AM, Doroshow JH, Fuchs C, Kiel K, Martin EW Jr, McGinn C, Petrelli NJ, Posey JA, Skibber JM, Venook A, Yeatman TJ; National Comprehensive Cancer Network. NCCN Practice Guidelines for Colorectal Cancer. *Oncology (Williston Park)* 2000; **14**:203-12.

17. Feneley MR, Partin AW. Diagnosis of localized prostate cancer: 10 years of progress. *Curr Opin Urol* 2000; **10**:319-27.

18. Harris LN, Liotcheva V, Broadwater G, Ramirez MJ, Maimonis P, Anderson S, Everett T, Harpole D, Moore MB, Berry DA, Rizzeri D, Vredenburgh JJ, Bentley RC. Comparison of methods of measuring HER-2 in metastatic breast cancer patients treated with high-dose chemotherapy. *J Clin Oncol* 2001; **19**:1698-706.

19. Rosell R, Morán T, Carcereny E, Quiroga V, Molina MA, Costa C, Benlloch S, Tarón M. Non-small-cell lung cancer harbouring mutations in the EGFR kinase domain. *Clin Transl Oncol* 2010; **12**:75-80.

20. Olaussen KA, Dunant A, Fouret P, Brambilla E, André F, Haddad V, Taranchon E, Filipits M, Pirker R, Popper HH, Stahel R, Sabatier L, Pignon JP, Tursz T, Le Chevalier T, Soria JC; IALT Bio Investigators. DNA repair by ERCC1 in non-small-cell lung cancer and cisplatin-based adjuvant chemotherapy. *N Engl J Med* 2006; **355**:983-91.

21. Matzke M, Matzke AJ, Kooter JM. RNA: guiding gene silencing. *Science* 2001; **293**:1080-3.

22. Ambros V. The functions of animal microRNAs. *Nature* 2004; **431**:350-5.

23. Bartel DP. MicroRNAs: genomics, biogenesis, mechanism, and function. *Cell* 2004; **116**:281-97.

24. Williams AE, Moschos SA, Perry MM, Barnes PJ, Lindsay MA. Maternally imprinted microRNAs are differentially expressed during mouse and human lung development. *Dev Dyn* 2007; **236**:572-80.

25. Lü J, Qian J, Chen F, Tang X, Li C, Cardoso WV. Differential expression of components of the microRNA machinery during mouse organogenesis. Biochem Biophys Res Commun. 2005; **334**:319-23.

26. Pasquinelli AE, Reinhart BJ, Slack F, Martindale MQ, Kuroda MI, Maller B, Hayward DC, Ball EE, Degnan B, Müller P, Spring J, Srinivasan A, Fishman M, Finnerty J, Corbo J, Levine M, Leahy P, Davidson E, Ruvkun G. Conservation of the sequence and temporal expression of let-7 heterochronic regulatory RNA. Nature 2000; **408**:86-9.

27. Dostie J, Mourelatos Z, Yang M, Sharma A, Dreyfuss G. Numerous microRNPs in neuronal cells containing novel microRNAs. *RNA* 2003; **9**:180-6.

28. Ishizuka A, Siomi MC, Siomi H. A Drosophila fragile X protein interacts with components of RNAi and ribosomal proteins. *Genes Dev* 2002; **16**:2497-508.

29. Shiohama A, Sasaki T, Noda S, Minoshima S, Shimizu N. Molecular cloning and expression analysis of a novel gene DGCR8 located in the DiGeorge

 ISSN 2330-4049

syndrome chromosomal region. *Biochem Biophys Res Commun* 2003; **304**:184-90.

30. Esquela-Kerscher A, Slack FJ. Oncomirs - microRNAs with a role in cancer. *Nat Rev Cancer* 2006; **6**:259-69.

31. Calin GA, Croce CM. MicroRNA signatures in human cancers. *Nat Rev Cancer* 2006; **6**:857-66.

32. Yanaihara N, Caplen N, Bowman E, Seike M, Kumamoto K, Yi M, Stephens RM, Okamoto A, Yokota J, Tanaka T, Calin GA, Liu CG, Croce CM, Harris CC. Unique microRNA molecular profiles in lung cancer diagnosis and prognosis. *Cancer Cell* 2006; **9**:189-98.

33. Calin GA, Ferracin M, Cimmino A, Di Leva G, Shimizu M, Wojcik SE, Iorio MV, Visone R, Sever NI, Fabbri M, Iuliano R, Palumbo T, Pichiorri F, Roldo C, Garzon R, Sevignani C, Rassenti L, Alder H, Volinia S, Liu CG, Kipps TJ, Negrini M, Croce CM. A MicroRNA signature associated with prognosis and progression in chronic lymphocytic leukemia. *N Engl J Med* 2005; **353**:1793-801.

34. Lu Y, Okubo T, Rawlins E, Hogan BL. Epithelial progenitor cells of the embryonic lung and the role of microRNAs in their proliferation. *Proc Am Thorac Soc* 2008; **5**:300-4.

35. Johnson CD, Esquela-Kerscher A, Stefani G, Byrom M, Kelnar K, Ovcharenko D, Wilson M, Wang X, Shelton J, Shingara J, Chin L, Brown D, Slack FJ. The let-7 microRNA represses cell proliferation pathways in human cells. *Cancer Res* 2007; **67**:7713-22.

36. Zhang B, Pan X, Cobb GP, Anderson TA. MicroRNAs as oncogenes and tumor suppressors. *Dev Biol* 2007; **302:1**-12.

37. Kent OA, Mendell JT. A small piece in the cancer puzzle: microRNAs as tumor suppressors and oncogenes. Oncogene 2006; **25**:6188-96.

38. Field RW, Smith BJ, Platz CE, Robinson RA, Neuberger JS, Brus CP, Lynch CF. Lung cancer histologic type in the surveillance, epidemiology, and end results registry versus independent review. *J Natl Cancer Inst* 2004; **96**:1105-7.

39. Stang A, Pohlabeln H, Müller KM, Jahn I, Giersiepen K, Jöckel KH. Diagnostic agreement in the histopathological evaluation of lung cancer tissue in a population-based case-control study. *Lung Cancer* 2006; 52:29-36.

40. Fabbri M, Garzon R, Cimmino A, Liu Z, Zanesi N, Callegari E, Liu S, Alder H, Costinean S, Fernandez-Cymering C, Volinia S, Guler G, Morrison CD, Chan KK, Marcucci G, Calin GA, Huebner K, Croce CM. MicroRNA-29 family reverts aberrant methylation in lung cancer by targeting DNA methyltransferases 3A and 3B. *Proc Natl Acad Sci USA* 2007; **104:**15805-10.

41. Takamizawa J, Konishi H, Yanagisawa K, Tomida S, Osada H, Endoh H, Harano T, Yatabe Y, Nagino M, Nimura Y, Mitsudomi T, Takahashi T. Reduced expression of the let-7 microRNAs in human lung cancers in association with shortened postoperative survival. *Cancer Res* 2004; **64**:3753-6.

42. Inamura K, Togashi Y, Nomura K, Ninomiya H, Hiramatsu M, Satoh Y, Okumura S, Nakagawa K, Ishikawa Y. let-7 microRNA expression is reduced in bronchioloalveolar carcinoma, a non-invasive carcinoma, and is not correlated with prognosis. *Lung Cancer* 2007; **58**:392-6.

43. Yu SL, Chen HY, Chang GC, Chen CY, Chen HW, Singh S, Cheng CL, Yu CJ, Lee YC, Chen HS, Su TJ, Chiang CC, Li HN, Hong QS, Su HY, Chen CC, Chen WJ, Liu CC, Chan WK, Chen WJ, Li KC, Chen JJ, Yang PC. MicroRNA signature predicts survival and relapse in lung cancer. *Cancer Cell* 2008; **13:**48-57.

44. Fazi F, Fontemaggi G .MicroRNAs and Lymph Node Metastatic Disease in Lung Cancer. *Thorac Surg Clin* 2012; **22**:167-75.

45. Wang YS, Wang YH, Xia HP, Zhou SW, Schmid-Bindert G, Zhou CC MicroRNA-214 Regulates the Acquired Resistance to Gefitinib via the PTEN/AKT Pathway in EGFR-mutant Cell Lines. *Asian Pac J Cancer Prev* 2012; **13**:255-60.

46. Chen X, Ba Y, Ma L, Cai X, Yin Y, Wang K, Guo J, Zhang Y, Chen J, Guo X, Li Q, Li X, Wang W, Zhang Y, Wang J, Jiang X, Xiang Y, Xu C, Zheng P, Zhang J, Li R, Zhang H, Shang X, Gong T, Ning G, Wang J, Zen K, Zhang J, Zhang CY. Characterization of microRNAs in serum: a novel class of biomarkers for diagnosis of cancer and other diseases. *Cell Res* 2008; **18**:997-1006.

47. García JM, García V, Peña C, Domínguez G, Silva J, Diaz R, Espinosa P, Citores MJ, Collado M, Bonilla F. Extracellular plasma RNA from colon cancer patients is confined in a vesicle-like structure and is mRNA-enriched. *RNA* 2008; **14:**1424-32.

 ISSN 2330-4049

48. Rabinowits G, Gerçel-Taylor C, Day JM, Taylor DD, Kloecker GH. Exosomal microRNA: a diagnostic marker for lung cancer. *Clin Lung Cancer* 2009; **10:42**-6.

49. Lawrie CH, Gal S, Dunlop HM, Pushkaran B, Liggins AP, Pulford K, Banham AH, Pezzella F, Boultwood J, Wainscoat JS, Hatton CS, Harris AL. Detection of elevated levels of tumour-associated microRNAs in serum of patients with diffuse large B-cell lymphoma. *Br J Haematol* 2008; **141**:672-5.

50. Mitchell PS, Parkin RK, Kroh EM, Fritz BR, Wyman SK, Pogosova-Agadjanyan EL, Peterson A, Noteboom J, O'Briant KC, Allen A, Lin DW, Urban N, Drescher CW, Knudsen BS, Stirewalt DL, Gentleman R, Vessella RL, Nelson PS, Martin DB, Tewari M. Circulating microRNAs as stable blood-based markers for cancer detection. *Proc Natl Acad Sci U S A* 2008; **105**:10513-8.

51. Ng EK, Chong WW, Jin H, Lam EK, Shin VY, Yu J, Poon TC, Ng SS, Sung JJ. Differential expression of microRNAs in plasma of patients with colorectal cancer: a potential marker for colorectal cancer screening. *Gut* 2009; **58**:1375-81.

52. Zhu W, Qin W, Atasoy U, Sauter ER. Circulating microRNAs in breast cancer and healthy subjects. *BMC Res Notes* 2009; **2**:89.

53. Taylor DD, Gerçel-Taylor C. Tumour-derived exosomes and their role in cancer-associated T-cell signalling defects. *Br J Cancer* 2005; **92**:305-11.

54. Lodes MJ, Caraballo M, Suciu D, Munro S, Kumar A, Anderson B. Detection of cancer with serum miRNAs on an oligonucleotide microarray. *PLoS One* 2009; **4**:e6229.

55. Hu Z, Chen X, Zhao Y, Tian T, Jin G, Shu Y, Chen Y, Xu L, Zen K, Zhang C, Shen H. Serum microRNA signatures identified in a genome-wide serum microRNA expression profiling predict survival of non-small-cell lung cancer. *J Clin Oncol* 2010; **28**:1721-6.

56. Hennessey PT, Sanford T, Choudhary A, Mydlarz WW, Brown D, Adai AT, Ochs MF, Ahrendt SA, Mambo E, Califano JA. Serum microRNA biomarkers for detection of non-small cell lung cancer. *PLoS One* 2012; **7**:e32307.

57. Bianchi F, Nicassio F, Veronesi G, di Fiore P. Circulating microRNAs: next-generation biomarkers for early lung cancer detection. *Ecancermedicalscience* 2012; **6**:246.

58. Shen J, Todd NW, Zhang H, Yu L, Lingxiao X, Mei Y, Guarnera M, Liao J, Chou A, Lu CL, Jiang Z, Fang H, Katz RL, Jiang F. Plasma microRNAs as potential biomarkers for non-small-cell lung cancer. *Lab Invest* 2011; **91**:579-87.

59. Rani S, Gately K, Crown J, O'Byrne K, O'Driscoll L. Global analysis of serum microRNAs as potential biomarkers for lung adenocarcinoma. *Cancer Biol Ther* 2013; **14**.

60. Xu T, Liu X, Han L, Shen H, Liu L, Shu Y. Up-regulation of miR-9 expression as a poor prognostic biomarker in patients with non-small cell lung cancer. *Clin Transl Oncol* 2013. **[In Press]**

61. Matsubara H, Takeuchi T, Nishikawa E, Yanagisawa K, Hayashita Y, Ebi H, Yamada H, Suzuki M, Nagino M, Nimura Y, Osada H, Takahashi T. Apoptosis induction by antisense oligonucleotides against miR-17-5p and miR-20a in lung cancers overexpressing miR-17-92. *Oncogene* 2007; **26**:6099-105.

62. Tavazoie SF, Alarcón C, Oskarsson T, Padua D, Wang Q, Bos PD, Gerald WL, Massagué J. Endogenous human microRNAs that suppress breast cancer metastasis. *Nature* 2008; **451**:147-52.

 ISSN 2330-4049

International Journal of Cancer Therapy and Oncology
www.ijcto.org

Laser photobiomodulation: A new promising player for the multi-hallmark treatment of advanced cancer

Luis Santana-Blank[1], Elizabeth Rodríguez-Santana[1], Heberto Reyes[1, 2, 3], Jesús A. Santana- Rodríguez [1], Karin E. Santana-Rodríguez[1]

[1]*Fundalas, Foundation for Interdisciplinary Research and Development, Caracas-Venezuela*
[2]*Hospital José María Vargas, Radiology Department, Caracas-Venezuela*
[3]*Clínica Ávila, Radiology Department, Caracas-Venezuela*

Received August 30, 2013; Revised September 2, 2013; Accepted September 3, 2013; Published Online September 4, 2013

Scientific Note

J. Watson, co-discoverer of the double helix structure of the DNA and a major force in cancer research over the last half century, has sharply criticized the War on Cancer on the following grounds: "Although the mortality from many cancers, particularly those of hematopoietic cells, has been steadily falling, the more important statistic may be that so many epithelial cancers (carcinomas) and effectively all mesenchymal cancers (sarcomas) remain largely incurable" [1]. Thus, Watson believes, that "the cancer world is not trying to cure incurable cancer. They need to concentrate on late-state disease " [1-2].

Indeed, efforts to increase awareness and screening have aimed to reduce late-stage disease and mortality. However, data show a significant increase in early-stages without a proportional decline in later ones [3]. Fortunately, most cancers do not progress to death. Still, cancer takes a heavy toll on society in terms of patient and family suffering, lost productivity and ever straining demands on public and personal finances. In this context, made worse by a "tsunami" of baby-boomers demanding more healthcare,[4] laser photobiomodulation (L-PBM), alone or combined with standard agents, may prove effective at targeting advanced cancer and other complex diseases safely and, potentially, at a low cost.

A major obstacle for many cancer drugs aiming at single molecular targets to minimizing nonspecific toxicity has been that clinical response is often transitory and followed by relapse [5]. In light of this, and given that the acquisition of new-generation cancer hallmarks is intricately linked and made possible by the tumor microenvironment, it has been suggested that new anticancer therapies should not aim at single molecular targets to solely kill cancer cells, but at re-establishing homeostasis-homeokinesis, a micro-environment effect which, as will be discussed below, may be induced by light [6].

L-PBM, also known as low-energy laser therapy (LLLT), refers to the use of monochromatic or quasi-monochromatic low-fluence light to induce primarily non-thermal photochemical effects. Skepticism surrounding this multidisciplinary field has been primordially rooted in a deep belief that, to affect biological systems, electromagnetic signals must ionize matter, or that too weak a signal may not be able to trigger biological effects[7]. Thus, a poor understanding of the physico-chemical basis of low-energy radiation and the fact that much initial research was methodologically flawed and came from behind the former Iron Wall deterred interest in the West for decades [8].

More than three hundred worldwide publications in reputed peer reviewed journals have turned this scenario. It has been demonstrated that L-PBM can stimulate or inhibit cellular function[9]. It has also been ascertained that signal and target characteristics determine biological outcome, which is optimal (or even positive) only within a narrow set of parameters. Nonetheless, until recently, there was great trepidation to explore L-PBM in cancer due to fear of increasing tumor cell proliferation[10-11].

Notwithstanding this, in cooperation with national and foreign research centers, our group completed animal testing and embarked on a phase I clinical trial in patients with advanced and progressive neoplasias using a singular low-energy infrared pulsed laser device (IPLD) that combines high-frequency ultrasound and near-infrared (NIR) radiation. Recruited patients, who suffered from advanced

Corresponding author: Luis Santana-Blank, MD;Fundalas Calle Las Flores con Guaraguao, C.C. Carabel PB Local 2, MUN 1262. Puerto La Cruz, Anzoátegui, Venezuela 6023-5; Email: luissantanablank@msn.com

Int J Cancer Ther Oncol, Vol. 1, No. 1, pp. 6-8, 2013.

ISSN 2330-4049

solid tumors, including epithelial cancers (carcinomas) and mesenchymal cancers (sarcomas), had exhausted available treatment alternatives and had a life expectancy ≥ 12 weeks (TNM IV- UICC).

After > 10 years of follow-up, the IPLD was found to be clinically safe and to improve performance status and quality of life. Antitumor activity was found in 88.23% of patients[12]. Immune data from the same trial showed modulation of CD4 CD45RA+, CD25, TNF-alpha, and soluble IL-2 receptor (sIL-2R),[13] in agreement with Coussens and others[14]. Also in accord with subsequent results by Tanaka et al., [15] the cytomorphology results of the trial showed selective activation of programmed cellular death (i.e., apoptosis, necrosis, anoikis) in neoplastic cells, but not in peripheral tissues. Microdensitometric T2-weighted MRI data further showed increased water content in tumor heterogeneities preceding tumor-volume reduction and therapeutic anticancer effects,[16] showing that changes in water-content acted as early predicator of tumor response in a manner consistent with the approach of Ross, Chenevert and others [17-18] for early tumor response determination.

Other studies show that L-PBM can trigger regenerative responses, alone or associated with stem cell therapy[19]. Epigenetic modulate chromatin structure, which affects gene transcription, [20] and L-PBM has been shown to reduce the frequency of chromosome aberrations[21]. Clinical results further suggest that L-PBM can cause phenotypic changes [22] consistent with theoretical data from a nonlinear DNA model, in which chaotic behaviors generated by damping, external fields and torque in solitone dynamics induce open states of the DNA which can regulate transcription and replication[23]. L-PBM has also shown effectiveness in the management of radiotherapy complications, such as mucositis [24].

Structural, kinetic, and thermodynamic implications of the above findings have been documented by our group[25-27]. In addition, we have proposed detailed mechanisms that complement the work of numerous authors, [28-30] and which help explain and substantiate one basic premise: that external electromagnetic energy (light) supplementation can enhance and even substitute for endogenous ATP production to power and modulate physiologically reparative mechanisms which can help reestablish homeostasis-homeokynesis, even when physiologic metabolic pathways have been compromised [31].

Recently, based on studies by Pollack and others on the exclusion zone (EZ), described as a fourth phase of water,[32] we hypothesized that the EZ might be targeted by L-PBM as an energy reservoir, which cells may use to fuel cellular work and trigger signaling pathways and gene expression in the presence of injury-induced redox potentials [31]. Nevertheless, we stressed that experimental proof that L-PBM would express effects via the EZ in a high-order biological system had not been attained. Now, clinical and experimental results which are remarkably consistent with the current understanding of the EZ are in press[33]. Such evidence, and the growing substantiation and reproduction of the above results, lead us to be confident that L-PBM will have a bright future in medicine at large, and oncology in particular.

A major goal for L-PBM in cancer is to safely control programmed cellular death and differentiation, as suggested by referred studies and in accord with the need for new multiple-hallmark cancer therapies. Challenges include determining optimal treatment parameters and further documenting the underlying mechanisms for potential applications in oncology. However, and given that laser-based technologies can be significantly less expensive than most cancer drugs, we hope that L-PBM may soon help to lower treatment costs whilst raising standard of care and quality of life, particularly, for the most vulnerable, such as the elderly, the poor and those suffering currently-untreatable late stage disease.

Competing interests

The authors declare that they have no conflicts of interest. The authors alone are responsible for the content and writing of the paper.

References

1. Watson J. Oxidants, antioxidants and the current incurability of metastatic cancers. *Open Biol* 2013; **3**: 120144.
2. Printz C. Is cancer research too conservative? Leaders weigh in on barriers to the fight against cancer. *Cancer* 2013; **119**: 1605-6.
3. Esserman LJ, Thompsom IM, Reid B. Overdiagnosis and Overtreatment in Cancer an Opportunity for Improvement. *Jama* 2013; [Epub ahead of print].
4. Lanzafame RJ. Photobiomodulation: an enlightened path emerges. *Photomed Laser Surg* 2013; **31**: 299-300.
5. Valastyan S, Weinberg RA. Tumor metastasis: molecular insights and evolving paradigms. *Cell* 2011;**147**: 275-92.
6. Santana-Blank L, Rodríguez-Santana E, Santana-Rodríguez JA, Santana-Rodríguez KE, Reyes H. Laser photobiomodulation as a potential multi-target anticancer therapy-review. *Journal of Solid Tumors* 2013; **3**: 50-62.
7. Del Giudice E, Guiliani L. Coherence in water and kT coherence in living matter. In: Non Thermal Effects and Mechanisms of Interaction Between Electromagnetic Fields and Living Matter. L. Giuliani, and M. Soffritti (eds.). Bologna, Italy: Ramazini Institute. *European Journal of Oncology Library* 2010 ; 7-23.

 ISSN 2330-4049

8. Basset CA. Fundamental and practical aspects of therapeutic uses of pulsed electromagnetic fields. *J Cell Biochem*. 1993; **51**: 387-93.
9. Lanzafame RJ. Philosophy, dogma, and possibilities. *Photomed Laser Surg* 2012; **30**: 403-4.
10. Lanzafame RJ. Photobiomodulation and cancer and other musings. *Photomed Laser Surg* 2011; **29**: 3-4.
11. Karu T. Mitochondrial mechanisms of photobiomodulation in context of new data about multiple roles of ATP. *Photomed Laser Surg* 2010; **28**: 159-60.
12. Santana-Blank LA, Rodríguez-Santana E, Vargas F, et al. Phase I trial of an infrared pulsed laser device in patients with advanced neoplasias. *Clin Cancer Res* 2002; **8**: 3082-91.
13. Santana-Blank LA, Castes M, Rojas ME, Vargas F, Scott-Algara D. Evaluation of serum levels of tumour necrosis factor-alpha (TNF-alpha) and soluble IL-2 receptor (sIL-2R) and CD4, CD8 and natural killer (NK) populations during infrared pulsed laser device (IPLD) treatment. *Clin Exp Immunol* 1992; **90**: 43-8.
14. Coussens LM, Zitvogel L, Palucka AK. Neutralizing Tumor-Promoting Chronic Inflammation: A Magic Bullet? *Science* 2013; **339**: 286-91.
15. Tanaka Y, Matsuo K, Yuzuriha S, Yan H, Nakayama J. Non-thermal cytocidal effect of infrared irradiation on cultured cancer cells using specialized device. *Cancer Sci* 2010; **101**: 1396-402.
16. Santana-Blank LA, Reyes H, Rodríguez-Santana E, Santana-Rodríguez KE. Microdensitometry of T2-weighted magnetic resonance (MR) images from patients with advanced neoplasias in a phase I clinical trial of an infrared pulsed laser device (IPLD). *Lasers Surg Med* 2004; **34**: 398-406.
17. Malyarenko DI, Ross BD, Chenevert TL. Analysis and correction of gradient nonlinearity bias in apparent diffusion coefficient measurements. *Magn Reson Med* 2013; [Epub ahead of print].
18. Malyarenko D, Galbán CJ, Londy FJ, et al. Multi-system repeatability and reproducibility of apparent diffusion coefficient measurement using an ice-water phantom. *J Magn Reson Imaging* 2013; **37**: 1238-46.
19. Abrahamse H. Regenerative medicine, stem cells, and low-level laser therapy: future directives. *Photomed Laser Surg* 2012; **30**: 681-2.
20. Costa FF. Epigenomics in cancer management. *Cancer Manag Res* 2010; **2**:255-65.
21. Joyce KM, Downes CS, Hannigan BM. Radioadaptation in indian muntjac fibroblast cells induced by low intensity laser irradiation. *Mutat. Res* 1999; **435**: 35-42.
22. Strohman R. Maneuvering in the complex path from genotype to phenotype. *Science* 2002; **296**: 701-3.
23. González JA, Martín–Landrove M, Carbo JR, Chacón M. Bifurcations and chaos of DNA solitonic dynamics, in: International Centre for Theoretical Physics bAU5 (eds.). Trieste, Italy: *International Atomic Energy Agency and United Nations Educational Scientific and Cultural Organization* 1994; 1-29.
24. Gautam AP, Fernandes DJ, Vidyasagar MS, Maiya AG, Nigudgi S. Effect of low-level laser therapy on patient reported measures of oral mucositis and quality of life in head and neck cancer patients receiving chemoradiotherapy--a randomized controlled trial. *Support Care Cancer* 2013; **21**: 1421-8.
25. Santana-Blank LA, Rodríguez-Santana E, Santana-Rodríguez KE. Photo-infrared pulsed bio-modulation (PIPBM): a novel mechanism for the enhancement of physiologically reparative responses. *Photomed Laser Surg* 2005; **23**: 416–424.
26. Santana-Blank L, Rodríguez-Santana E, Santana-Rodríguez KE. Theoretic, experimental, clinical bases of the water oscillator hypothesis in near-infrared photobiomodulation. *Photomed Laser Surg*.2010; **28**: S41–52.
27. Santana-Blank L, Rodríguez-Santana E, Santana-Rodríguez KE. Photobiomodulation of aqueous interfaces as selective rechargeable bio-batteries in complex diseases: personal view. *Photomed Laser Surg* 2012; **30**: 242-249.
28. Karu T. Mitochondrial mechanisms of photobiomodulation in context of new data about multiple roles of ATP. *Photomed Laser Surg*. 2010; **28**: 59-60.
29. Myakishev-Rempel M, Stadler I, Brondon P. et al. A preliminary study of the safety of red light phototherapy of tissues harboring cancer. *Photomed Laser Surg* 2012; **30**: 551-8.
30. Tata DB, Waynant RW. Laser therapy: A review of its mechanism of action and potential medical applications. *Laser & Photonics Review* 2011; **5**: 1-12.
31. Luis Santana-Blank, Elizabeth Rodríguez-Santana, Jesús A. Santana-Rodríguez, Karin E. Santana-Rodríguez, Solid tumors and photobiomodulation: A novel approach to induce physiologically reparative homeostasis/homeokinesis-review. *Journal of Solid Tumors* 2012; **2**: 23-35.
32. Pollack GH. The Fourth Phase of Water: Beyond Solid, Liquid, and Vapor. 1st ed. Seattle, WA: Ebner and Sons Publishers; 2013.
33. Santana-Blank L, Rodríguez-Santana E, Santana-Rodríguez JA, Santana-Rodríguez KE. Photobiomodulation of Aqueous Interfaces: Finding Evidence to Support the Exclusion Zone in Experimental and Clinical Studies. *Photomedicine & Laser Surgery* 2013; In Press.

 ISSN 2330-4049

International Journal of Cancer Therapy and Oncology
www.ijcto.org

Robotic Cystectomy : Important considerations before commencing the procedure independently

Nikhil Vasdev, Ben Lamb, Tim Lane, Gregory Boustead, James M Adshead

Hertfordshire and South Bedfordshire Urological Robotic Centre, Department of Urology, Lister Hospital, Stevenage, UK

Received September 03, 2013; Accepted September 18, 2013; Published Online September 20, 2013

Scientific Note

A radical cystectomy (RC) with pelvic lymph node dissection (PLND) is the gold standard for the management of the appropriately selected patient with muscle invasive bladder cancer (MIBC) and non-muscle invasive bladder cancer (NMIBC)/carcinoma in situ (CIS) who fail appropriate intravesical therapy. In the last decade, Robotic Radical Cystectomy (RRC) is being performed in a large number of international Centre's with the published advantages of decreased blood loss, improved post-operative convalescence and earlier initiation of adjuvant therapy[1] when compared to open cystectomy (OC). Current literature indicates that a RC is equivalent to OC from the oncological perspective. An OC is associated with high rates of morbidity (19-64%) or mortality (6-11%), although there is a wide variation in current literature.[1-11] A RRC is perhaps just one modality in a raft of measures to try reducing mortality and morbidity of a cystectomy.

To the Robotic Urological Surgeon, a RRC comes with numerous specific challenges. Questions that arise at the time of commencing a RRC include the learning curve of the procedure, learning steps to enhances ones speed to perform the procedure efficiently and safely, level of lymphnode dissection, whether one should embark of performing an intracorpealileal conduit or neobladder formation and the cost of commencing a RRC service. The patient's postoperative management is the most important step to ensure that the post-operative complications are kept to a minimum using a multi-disciplinary team (MDT) approach.

Corresponding author: Nikhil Vasdev, FRCS (Urol); Hertfordshire and South Bedfordshire Urological Robotic Centre, Department of Urology, Lister Hospital, Stevenage, UK.
Email: nikhilvasdev@doctors.org.uk

Cite this article as:
Vasdev N, Lamb B, Lane T, Boustead G, Adshead J. Robotic Cystectomy : Important considerations before commencing the procedure independently. Int J Cancer Ther Oncol 2013;**1**(1):01017.
DOI: 10.14319/ijcto.0101.7

In current literature high volume centers with experienced surgeons have reported patient outcomes that are acceptable from the perspective of extended pelvic lymph node dissection, positive surgical margin rates and highlight that patients are not being compromised from the surgical perspective in undergoing a RC.[2]

The learning curve of a RRC is not as clearly defined in comparison to Robotic Radical Prostatectomy (RRP). Before commencing aRRC it is important to be proficient and familiar with robotic pelvic surgery. Most robotic surgeons are proficient in RRP before embarking on performing independent RRC. Hayn *et al*.[3] have indicated that an acceptable level of proficiency to perform a RRC is established after the 30th case by measuring post-operative parameters such as operative time, lymph node yield (LNY), estimated blood loss (EBL), and margin positivity. At our center we commenced performing RC after performing 150 Robotic RRP. We would strongly recommend that a robotic urological surgeon who is keen to commence Robotic RC should be proficient in robotic RRP and in performing an extended pelvic lymph node dissection (EPLND). A well-trained Robotic Team consisting of the lead experience console surgeon, experienced assistant, nursing staff and an experience anesthetist is essential for the commencement of a RRC program. The techniques that a team needs to develop to aid in improving intra-operative times including a fast docking/ undocking time, piggyback techniques for ports and , the use of different specimen retrieval bags, use of laparoscopic staplers and new intraoperative hemostatic agents.

Whilst performing an adequate RRC involves the removal of the bladder, the importance of performing an EPLND cannot be understated. There is no defined lymph node dissection template for a RRC and some centers now perform an EPLND before performing the robotic cystectomy during a RRP.[4] The anatomical landmark that we recommend to be followed is up to the level of the aortic bifurcation or the Inferior mesenteric artery (IMA), lymph node of cloquet distally, genitofemoral nerve laterally and perivesical tissue laterally. Using this template the surgeon will be able to excise the external iliac, obturator, hyogastic and common

 ISSN 2330-4049

iliac. Some authors[5] recommend the excision of the presacrallymphnode as the excision of this lymph node group facilitates the transposition of the left ureter behind the sigmoid mesentery to aid in intracorporeal anastomosis.

With an evolution in robotic systems there has been an increase in the number of patients undergoing intracorporeal ileal conduit and neobladder formation. The excellent technical description of the procedure has led to the adoption of these techniques worldwide.[5] We have recently published the results of our initial patients.[6] Robotic surgeons must be proficient in the performing the cystectomy part of the RRC before embarking on either an intracorporeal ileal conduit or neobladders formation due the complications of keeping patients in the steep Trendelenburg position for prolonged periods, which include compartment syndrome, neurological complications, intraocular complications, and rhabdomyolysis.[7,8] Recent evidence from high volume centres performing RRC and intracorporeal neobladders diversion confirm that initial results are comparable to contemporary open series with regards to complication rates, functional and oncological outcomes.[9] We recommend that a surgeon should embark on performing an intracorporeal ileal conduit and neobladder formation only if the ablative part of RRC is less than 2.5 hours of total operative time. If the ablative times are longer we recommend performing a mini-laparotomy for excision of the cystectomy specimen and completing an extracorporeal ileal conduit or neobladders.[6]

The cost effectiveness of a RRC when compared to an open radical cystectomy (ORC) has a disadvantage of being more expensive due to the initial high purchase and maintenance contract cost, although when the indirect costs of complications and extended hospital stay with ORC are considered, RRC may be less expensive than the traditional open procedure. In order to accurately evaluate the cost effectiveness of RARC versus ORC, prospective randomized trials between the two surgical techniques with long-term oncologic efficacy are needed.[10]

In conclusion, a RRC with intracorporeal ileal conduit or neobladders formation is a complex robotic procedure that should only be undertaken by an experienced robotic pelvic oncological surgeon who is completely competent at performing a RRP + EPLND. A carefully mentored approach and a well-trained robotic team are the two key components to make the procedure a success.

Competing interests

The authors declare that they have no conflicts of interest. The authors alone are responsible for the content and writing of the paper.

References

1. Liss MA, Kader AK. Robotic-assisted laparoscopic radical cystectomy: history, techniques and outcomes. *World J Urol* 2013 ; **31** :489-9.
2. Khan MS, Elhage O, Challacombeet al B. Long-term outcomes of robot-assisted radical cystectomy for bladder cancer. *Eur Urol* 2013; **64**: 219–224.
3. Hayn MH, Hussain A, Mansour AM et al. The learning curve of robot-assisted radical cystectomy: results from the International Robotic Cystectomy Consortium. *Eur Urol* 2010; **58**: 197-202.
4. Desai MM, Berger AK, BrandinaRRet al. Robotic and laparoscopic high extended pelvic lymph node dissection during radical cystectomy: technique and outcomes. *Eur Urol* 2012; **61**: 350-5.
5. Pruthi RS, Nix J, McRackan D, et al. Robotic-assisted laparoscopic intracorporeal urinary diversion. *Eur Urol* 2010; **57**: 1013–21.
6. Bishop C, Vasdev N, Boustead G, Adshead JM. Robotic IntracorpealIleal conduit formation – Initial experience from a single UK centre. *Advances in Urology* [Article in press].
7. Mattei A, Di Pierro GB, Rafeld V, Konrad C, Beutler J, Danuser H. Positioning injury, rhabdomyolysis, and serum creatine kinase-concentration course in patients undergoing robot-assisted radical prostatectomy and extended pelvic lymph node dissection. J Endourol 2013; **27**: 45-5.
8. Pandey R, Garg R, Darlong V, Punj J, Chandralekha, Kumar A. Unpredicted neurological complications after robotic laparoscopic radical cystectomy and ileal conduit formation in steep trendelenburg position: two case reports. *ActaAnaesthesiol Belg* 2010; **61**: 163-6.
9. Tyritzis SI, Hosseini A, Collins J, Nyberg T, Jonsson MN, Laurin O, Khazaeli D, Adding C, Schumacher M, Wiklund NP. Oncologic, Functional, and Complications Outcomes of Robotic assisted Radical Cystectomywith Totally Intracorporeal Neobladder Diversion. *Eur Urol* 2013 (Article in press).
10. Mmeje CO, Martin AD, Nunez-Nateras R, Parker AS, Thiel DD, Castle EP. Cost analysis of open radical cystectomy versus robot-assisted radical cystectomy. *Curr Urol Rep* 2013;**14**: 26-3.
11. Prentis JM, Trenell MI, Vasdev N, French R, Dines G, Thorpe A, Snowden CP. Impaired cardiopulmonary reserve in an elderly population is related to postoperative morbidity and length of hospital stay after radical cystectomy. *BJU Int* 2013; **112**: E13-9.

 ISSN 2330-4049